

ELECTROCHEMICAL STUDIES AND APPLICATIONS OF
TRIS[5-AMINO-1,10-PHENANTHROLINE]Fe[II]
POLYMERIC-FILM-COATED GLASSY-
CARBON ELECTRODES

BY

JIANBO YU

Bachelor of Science

Shandong University

Jinan, Shandong

P. R. China

1984

Submitted to the Faculty of the
Graduate College of the
Oklahoma State University
in partial fulfilment of
the requirements for
the degree of
DOCTOR OF PHILOSOPHY
July, 1991

ELECTROCHEMICAL STUDIES AND APPLICATIONS OF
TRIS[5-AMINO-1,10-PHENANTHROLINE]Fe[II]
POLYMERIC-FILM-COATED GLASSY-
CARBON ELECTRODES

Thesis Approved:

Horacio A Mottola

Thesis Adviser

Ziad El Raus

Paul W. Glueck

P. M. ...

Norman D. ...

Dean of the Graduate College

ACKNOWLEDGEMENTS

I wish to express my sincere appreciation to my advisor: Dr. Horacio, A. Mottola for not only his intelligent guidance and support during my graduate career, but also his patience and understanding. I also thank Drs. EL Rassi, P. Geno and H. A. Melouk for serving as members of my graduate committee Their suggestions and support were very helpful..

TO many of my good friends and colleagues : Sun gang, Sudha, Terry, Patricia, Chris and Dale, Thank you all very much for your friendship and help.

I am grateful for the financial support provided by the U. S. Department of Energy and Oklahoma State University.

Finally, I would like to thank my parents, Jingchao Yu and Guiqing Pai, and my husband Huadong Gai for their support during my graduate career, and especially to my son, luyang, who has been the real inspiration to my study.

TABLE OF CONTENTS

Chapter	Page
I. INTRODUCTION.....	1
II. CHEMICALLY MODIFIED ELECTRODES BY ELECTROCHEMICAL POLYMERIZATION: A REVIEW.....	8
Chemically Modified Electrode.....	8
Polymer-film-coated Electrodes.....	9
Electrochemically Polymerized Redox Films...14	14
Pyrrole-substituted Complexes.....16	16
Complexes with Vinyl-substituted Polypyridyl Ligands.....	19
Complexes with aromatic amino-substituted ligands.....	20
Electrochemical Properties of Redox Film-coated Electrodes.....	21
Conclusions.....	25
III. ELECTROOXIDATIVE POLYMERIZATION OF TRIS[5-AMINO-1-10-PHENANTHROLINE] IRON(II) ON GLASSY CARBON.....	27
Experimental.....	27
Apparatus.....	27
Reagents and Solutions.....	27
Results and Discussion.....	28
Electrochemical Behavior of 5-Amino-1,10- phenanthroline.....	28
Electrooxidative Polymerization of Tris[5-amino-1,10-phenanthroline]iron[II]...30	30
Effects of Scanning Rate on the Cyclic Voltammogram Obtained with the Polymer Film- coated Glassy-Carbon Electrode.....	34
IV. SOME BASIC PROPERTIES OF POLYMER-MODIFIED ELECTRODES.....	38
Experimental.....	38
Apparatus.....	38
Reagents and Solutions.....	39
Procedures	
Results and Discussion.....	41
Electron Scanning Micrograph.....	41
UV-visible Spectra.....	41

Chapter	Page
Infrared Spectra.....	50
V. EFFECT OF COUNTERIONS IN TRIS[5-AMINO-1,10-PHENANTHROLINE]IRON[II]-FILM-COATED GLASSY-CARBON ELECTRODES.....	54
Experimental.....	54
Reagents and Solutions.....	54
Procedures.....	55
Results and Discussion.....	55
Cyclic Voltammetry.....	55
Hydration Process.....	58
Effects in NO ₂ (g) Detection.....	63
Conclusions.....	64
SOME APPLICATIONS OF ELECTRODES MODIFIED WITH POLYMERIC TRIS[5-AMINO-1,10-PHENANTHROLINE]IRON[II].....	66
Experimental.....	66
Apparatus.....	66
Reagents and Solutions.....	70
Results and Discussion.....	70
Determination of NO ₂ (g).....	70
Response to NO ₂ (g).....	70
Effect of Polymer Thickness.....	74
Effect of pH of Carrier Solution.....	77
Effect of Carrier Flow Rate and Injected Sample Size.....	79
Sensitivity, Limit of Detection, Dynamic Range and Stability.....	82
Determination of Phenol, Cl ₂ , H ₂ S, SO ₂	85
Response to Phenol.....	85
Response to Halogens.....	87
Response to Hydrogen Sulfide and Sulfur Dioxide.....	91
VII. CONCLUSIONS.....	95
REFERENCES.....	97

LIST OF TABLE

Table	Page
1. Methods Used for Chemically Modified Electrode Preparation.....	10
2. Methods of Making Polymeric Films.....	15
3. Pyrrole-based Polymer Films Formed by Electropolymerization.....	18
4. Absorption Wavelength for Peaks in the UV-visible Region.....	42
5. Peak Current from Cyclic Voltammograms, Hydration Rate of the Film, Shifts in Peak Potential, Responses to NO ₂ Injections in Different Carrier Solutions.....	57
6. Relationship between the Thickness of Electrodeposited Polymer and the Response to Injected NO ₂	75
7. Repetitive Response of a Polymer-modified Electrode to 18 pp (v/v) NO ₂	86

LIST OF FIGURES

Figure	Page
1. Calibration Curve for SO ₂ Determination on Modified and Unmodified Glassy-carbon Electrodes.....	3
2. Sketch of Electron Hopping at a Polymer-modified Electrode-.....	12
3. Repeated Cyclic Voltammograms of a 0.030 mM Solution of Tris[5-amino-1,10-phenanthroline]Fe(II) in Acetonitrile at a Glassy-carbon Electrode-.....	31
4. Cyclic Voltammograms Obtained with a Polymer-Coated Electrode in 0.10 M NaClO ₄ . Scan Rate 50 mV s ⁻¹	32
5. Reduction Peak Currents as a Function of Cycle Number.....	33
6. Peak Current vs Square Root of Scan Rate Plot.....	35
7. Difference in Peak Potentials vs Square Root of Scan Rate Plot.....	37
8. Scanning Electron Micrograph of a Naked Wax-paste Electrode.....	43
9. Scanning Electron Micrograph of a Polymer-coated Wax-paste Electrode.....	44
10. X-ray Analysis Diffraction Pattern of a Polymer-coated Wax-paste Electrode.....	45
11. UV-visible Absorbance Spectrum of Polymer/DMF Solution.....	46
12. UV-visible Absorbance Spectrum of Complex/DMF Solution.....	47
13. UV-visible Absorbance Spectrum of Precipitate/DMF Solution.....	48

Figure	Page
14. UV-visible Absorbance Spectrum of 5-amino-1,10-phenanthroline/DMF Solution.....	49
15. IR Spectrum of Polymer in KBr.....	51
16. IR Spectrum of Complex in KBr.....	52
17. Cyclic Voltammograms of Film-coated Electrode in 0.10 M HCOO ⁻ Aqueous Solution.....	60
18. Cyclic Voltammograms of Film-coated Electrode in 0.10 M Pic ⁻ Aqueous Solution.....	61
19. Cyclic Voltammograms of Film-coated Electrode in 0.10 M ClO ₄ ⁻ Aqueous Solution.....	62
20. Block Diagram of the Thin-layer Cell Machined out of Kel-F Material.....	67
21. Configuration of Apparatus for Continuous-flow Determination of NO ₂	69
22. Hydrodynamic Voltammogram Showing the Responses to NO ₂	71
23. Typical Transient Signals due to NO ₂ Injections.....	73
24. Idealized Structural Representation of the Polymer-coated Glassy-carbon Electrode.....	76
25. Effect of pH on Signal Height for NO ₂ Determination.....	78
26. Effect of Carrier Flow Rate on Signal Height for NO ₂ Determination.....	81
27. Effect of Sample Size on Signal Height for NO ₂ Determination.....	83
28. Dependence of Signal Height on Concentration of Injected NO ₂	84
29. Calibration Curve for Phenol Determination on Modified Glassy-carbon Electrode.....	88
30. Calibration Curve for Phenol Determination ⁹ on Modified Glassy-carbon Electrode.....	89

Figure	Page
31. Hydrodynamic Voltammogram for $\text{Cl}_2(\text{g})$	90
32. Hydrodynamic Voltammogram for $\text{H}_2\text{S}(\text{g})$	92
33. Hydrodynamic Voltammogram for $\text{SO}_2(\text{g})$	93

CHAPTER I

INTRODUCTION

Since the first dropping mercury electrode was used as a probe for chemical detection [1], there has been an extensive development of different types of electrodes as well as studies of their applications. Along with the success with these electrodes, some difficulties were encountered, such as slow electron transfer rate or easily poisoned surfaces. Because of these difficulties, efforts have been made to seek some kind of chemical modification of the electrode surface that would minimize these shortcomings. The term "chemically modified electrode" refers to any electrode for which the surface region has been chemically tailored to provide properties different from those available on any surface of the electrode material itself. Because of the modification process, the electron transfer can be either accelerated or slowed down as desired. Also the electrode surface can be protected from poisoning. Chemically modified electrodes have received considerable attention during the last fifteen years, largely because they have a wide range of potential applications in electrochemical technology, and especially in chemical analysis. Electrodes have been

modified in a number of ways; mainly by covalent bonding, by direct admixing or by electrochemical polymerization [2].

Electrochemical polymerization has some unique advantages: a. it is easy to perform; b. it provides a stable and uniform modified surface; c. it offers the possibility of a more efficient electrochemical catalysis; d. it can protect the electrode surface from poisoning.

Chemical modification has been performed on almost every possible electrode surface including glassy carbon. Glassy carbon has found extensive use in voltammetry in the last twenty years because of a low residual current over a wide potential range and relatively high sensitivity in detection [3]. Because of its porous structure, however, the surface can easily be saturated and poisoned with analyte or product of the electrochemical reaction in a short period of time. In addition the electron transfer rate is somehow sluggish when compared to that at metal electrodes. Figure 1 illustrates the poisoning problem with an example for the determination of SO_2 . After a few determinations, the calibration curve reaches a plateau for a bare surface since the electrode surface has been totally covered by the analyte. Because of these characteristics, glassy carbon electrodes have received considerable attention with regard to modification.

Although chemically modified electrodes have attracted considerable attention, few bonafide analytical applications have been reported.

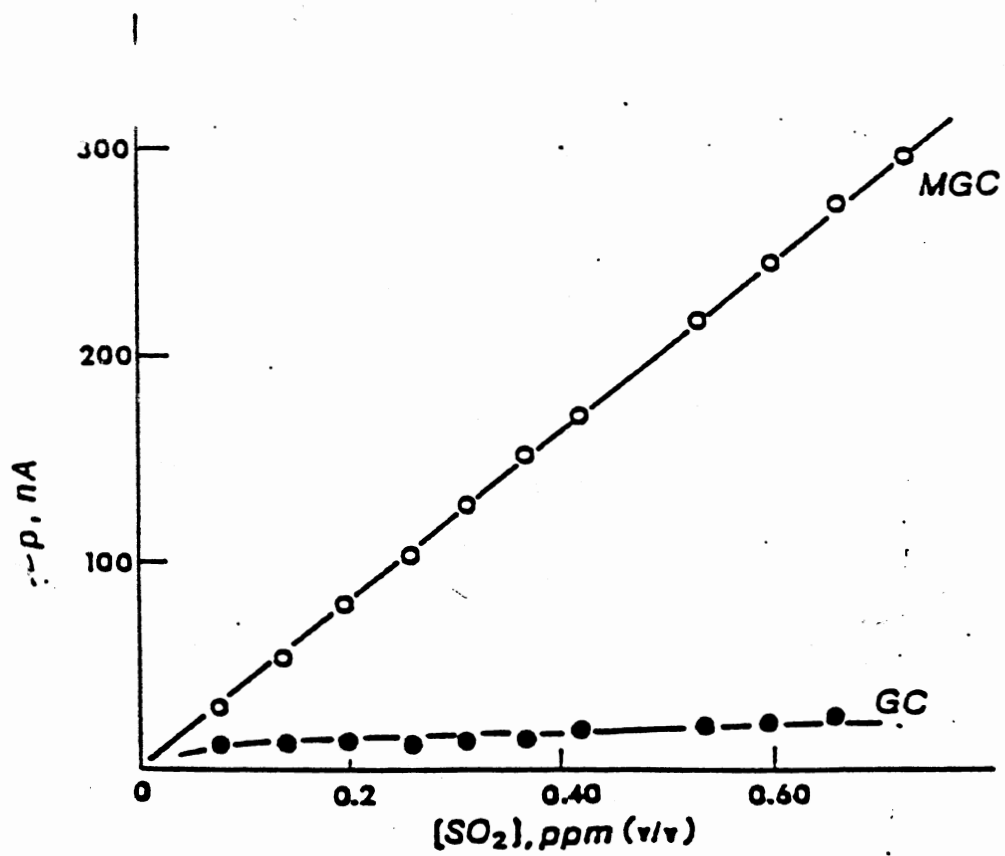


Figure 1. Calibration Curve of $SO_2(g)$ Determination on Modified (MGC) and Unmodified (GC) Glassy Carbon Electrodes [81]

Nitrogen dioxide has been of real concern in analytical and environmental chemistry because of its relevance to air pollution. The analytical methods generally used for the determination of NO_2 [4,5,6] involve gasometric procedures, absorption in liquids and subsequent determinations by titration, spectrophotometry, infrared spectroscopy, gas chromatography, or mass spectrometry. These methods are often time-consuming, elaborate, require expensive equipment, or have poor limits of detection. Electrochemical analysis potentially offers very competitive limits of detection with relatively simple instrumentation. The oxidation and reduction of NO_2 at a metallized membrane electrode can be employed for the determination of this gaseous species [7]. Nitrogen dioxide, however, has the tendency to poison the electrode surfaces and thus cause poor reproducibility. From a practical viewpoint a glassy-carbon electrode coated with a polymer film can be ideal for use in the electrochemical determination of NO_2 because of: 1. Protection of the electrode surface from fouling; 2. Increase in electrochemical reaction rate; 3. Enhancement of selectivity and sensitivity; 4. Relatively inexpensive implementation.

Implementation in a continuous-flow system makes the idea even more attractive because of the additional convenience of continuous detection and high sampling rate.

The work reported in this thesis is focused on the construction and use of a chemically modified glassy carbon electrode made by electrochemical polymerization to produce a

thin film of tris[5-amino-1,10-phenanthroline]iron[III] complex. The resulting modified electrode has been electrochemically and spectrometrically characterized, and applied to the determination of redox gaseous pollutants in air samples.

A diffusionally controlled process in electron transfer across the polymeric film on the electrode surface was electrochemically observed. In addition, some structural information on the polymer film has been obtained by use of infrared, UV-visible and x-ray spectroscopy. The determination of nitrogen dioxide was performed in a continuous-flow system with the polymer-film-coated electrode as a probe. Phenol, another common pollutant in waste water, also was determined with the same system.

The application of modified electrodes is very important from a practical point of view. However, in order to obtain a theoretical direction for such applications, it is also necessary to try to understand the working mechanism of the modified electrode response. That is why the dynamics of electron transport at the modified electrode has received attention [8]. Part of the research reported in this thesis was dedicated to evaluate the effect of counter-ions on the cyclic voltammetric response and in the amperometric determination of NO_2 , with the hope of singling out the rate-determining step in the overall electron transfer process as well as obtaining criteria for the selection of supporting electrolyte in the determination of certain analytes.

An attempt was also made to develop other redox couples for the growth of polymer films on glassy-carbon electrodes, such as Co(II/III) and Cu(I/II) as 5-amino-1,10-phenanthroline complexes. Unfortunately it was not possible to obtain a stable polymer film on the electrode surface. In case of the complex with cobalt, two pairs of major peaks were observed in the cyclic voltammograms. One of the peak currents, however, decreased as the number of cycles increased and the other one increased at the same time. Both decrease and increase, however, were very small after a few cycles and remained the same after 20 cycles.

With careful rinsing, a yellowish film was observed on the electrode surface. Several problems were observed, however, namely:

1. The polymer dissolved rapidly if immersed in a blank supporting electrolyte solution.

2. Growth of the polymer film was not reproducible.

Consequently, no electrochemical study was pursued on this. There are reports that such polymers with Co(II/III) can be grown [20], but it was observed that:

1. A smaller faradaic efficiency operates in the polymerization of the cobalt complex when compared with that of the iron complexes.

2. A substantial decrease in peak current was observed in cyclic voltammograms when the polymer electrode was immersed in blank supporting electrolyte solution.

In the case of copper complexes, the attempt was equally fruitless.

In summary, this thesis is composed of the following parts:

1. The polymer-film-coated glassy-carbon electrode made from tris[5-amino-1,10-phenanthroline]Fe[II] complex was studied both photometrically and electrochemically. A diffusion-controlled process in electron transfer across the polymeric film was electrochemically observed. Some structural information of the polymer was obtained from UV-visible spectra, infrared spectra, and electron scanning microscopy.

2. Determinations of NO_2 , phenol, SO_2 , H_2S , and Cl_2 were accomplished in a continuous-flow system using the polymer-film-coated electrodes as detectors. Very competitive limits of detection were obtained in the cases of NO_2 and phenol and some necessary experimental parameters were optimized.

3. The effects of the counter-ion were tested by cyclic voltammetry and also in the amperometric determination of nitrogen dioxide. Explanations are given to account for the observed behaviors.

CHAPTER II

CHEMICALLY MODIFIED ELECTRODES BY ELECTROCHEMICAL POLYMERIZATION:

A REVIEW

Chemically Modified Electrodes

In electrochemistry there has long been an interest in the adsorption phenomenon and in the modifications resulting from such adsorption of ions and molecules on the electrode surface. An adsorbed layer of molecules or ions can accelerate or slow down the rate of electron transfer. There is a difference, however, between encountering unexpected adsorption and deliberately seeking to immobilize chemicals on the electrode surface to achieve some practical goals. The earliest research on the attachment of chemical species involved irreversibly adsorbing monolayers or submonolayers of electroactive reagents onto the electrode material. Lane and Hubbard [9] demonstrated this pathway in their pioneering experiments with quinone-bearing olefins chemisorbed on platinum. Murray et. al. [10] covalently bonded several ligands (amine, pyridine, and ethylenediamine) to tin oxide surfaces. Since then, for more than two decades, the development of chemically modified electrodes has received continued attention [11,12]. The main idea behind chemically

modified electrodes is to immobilize a chemical on an electrode surface so that the electrode thereafter displays the chemical, electrochemical, optical and other physicochemical properties of the immobilized species.

Methods for immobilizing chemical reagents on electrode surfaces are summarized in Table 1 along with corresponding references.

Polymer Film-coated Electrodes

The formation of polymer films on electrode surfaces and the use of polymer-coated electrodes for analytical purposes have been known for some time. The distinctive characteristic of modern polymer-coated electrodes is that the polymer films contain electrochemically and/or chemically reactive implanted centers. The electroactive center can undergo electron transfer reactions with the electrode and, since the polymer film generally contains the equivalent of many monomolecular layers worth of electroactive sites, their electrochemical responses are larger and more easily observed than those of immobilized monomolecular layers. The quantities of the electroactive sites are in the range of 10^{-10} to 5×10^{-6} mol.cm⁻² (4).

The popularity of multimolecular electroactive polymer films is due not only to the reasons mentioned above, but also to other factors:

TABLE 1

METHODS USED FOR CHEMICALLY
MODIFYING ELECTRODES

Chemisorption of reagent
on platinum surface [9]
on carbon surface [13]
on mercury surface [14]
on gold surface [15]

Formation of covalent bond between electrode and electroactive reagent
at metal oxide surfaces [16]
at carbon surfaces [17]

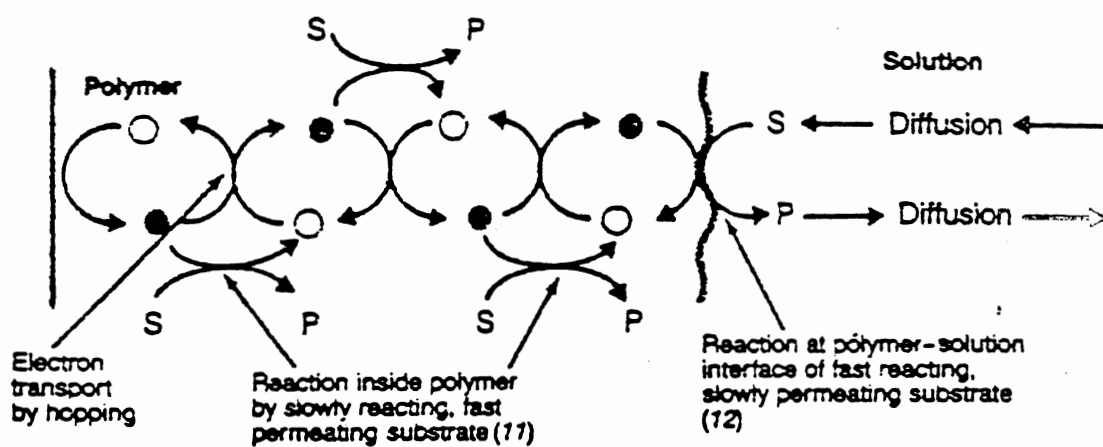
Polymer film coatings on electrodes
redox polymers [18-21]
ion exchange (electrostatically trapped) [22,23]
electronically conducting polymers [24]

Heterogeneous multimolecular layers
modifying agent mixed with carbon paste [25]
clay-modified [26]
electroactive particles in electroactive polymer [27]

1. They are technically easier to apply to electrode surfaces than films covalently attached.
2. Their electrocatalytic efficiency is enhanced.
3. They can serve as preconcentrating media or as transport barriers.
4. They are generally stable.

Electroactive polymer films are intrinsically conductive of both ions and electrons. According to their conduction mechanism, they are classified as redox polymers, electronically conductive polymers (organic metals), and ion-exchange polymers.

Redox polymer films are electroactive ones that contain electron donor and acceptor sites as part of the polymer backbone. Oxidation and reduction of fixed sites introduce charged sites into the polymer film, which then, to achieve charge neutrality, require the transport of counterions from or into the contacting electrolyte solution. Electron hopping (electron self-exchange; see Figure 2) is believed to be the mechanism for electron transport [4,33], but it is possible that the counterion motions can control, partially or totally, the rate of charge transport [4,33]. Aside from such control, a redox polymer undergoing electrolysis may follow Fick's diffusion law and actually the usual Fick's formalism agrees with the experimental results [33]. Thus the rate of charge transport is usually characterized by an apparent diffusion coefficient (D) which can vary over several orders of magnitude



Mediated electrocatalysis by a redox polymer film

S: substrate; P: product

Figure 2. Sketch of Electron Hopping at a Polymer-modified Electrode

for known electroactive polymers (10^{-10} - 10^{-7} cm² s⁻¹) [34].

Electronically conductive polymers such as polyacetylene and polypyrrole are supposed to behave as metallic matrices without any diffusion control. In some cases, a conducting mechanism is suggested in which charge transport is that of oxidation (charging) or reduction (discharging) of the polymer itself [35]. The active sites are operationally defined as those segments of polymer chains that interchange electrons in the redox reactions. In the conducting state, the materials are ionic and the conductivity is higher along the chain direction. Conducting polymers can be broadly divided into two types, those with a degenerate ground state and solitons to mediate excitations and those where the ground state degeneracy is lifted so that polarons and bipolarons mediate excitations and the dominant charge-storage configurations. Polyacetylene is an extensively studied example with a degenerate ground state. Polypyrrole, on the other hand, has a nondegenerate ground state [36].

Ion-exchange polymer films are made electroactive by exchange of some of their charge-compensating counterions. An example is exchanging $\text{Fe}(\text{CN})_6^{4-}$ for the ClO_4^- counterion of a protonated poly[vinylpyridine] film [77]. The main efforts of research done on ion exchange polymers have been focused on two types of films: perfluoro ion exchange polymers [37] and polypyrrole-based ion exchange polymers [23]. Perfluoro ion exchange polymers are very useful

materials with various applications in electrochemistry. These polymers retain the outstanding chemical stability of the perfluorinated polymeric backbone, and moreover show ion exchange capability, good electrical conductivity in contact with electrolytes, and also some solubility in organic solvents. This solubility enables the preparation of stable polyelectrolyte films on electrodes by dip-coating or by evaporation of the solution on the electrode surface. The most important characteristic of polypyrrole ion exchange polymers is the high electronic conductivity, while the perfluoro polymers show high ionic conductivity. Several groups have prepared composite films of polypyrrole and Nafion. These films combine the high electronic conductivity of polypyrrole and the high ionic conductivity of Nafion (Nafion is a perfluorinated polymer produced by E. I. DuPont de Nemours and Co.) [38,39].

Electrochemically Polymerized Redox Films

Electrochemically active polymer films have been formed in many ways. The preparation methods can be either physical or chemical. Most of the popular methods used are listed in Table 2. Among all the methods listed in Table 2, electrochemical polymerization is the most satisfactory one, mainly for two reasons:

1. The stability of the film produced.
2. The simplicity of the instrumentation required and the procedures needed to form the film.

TABLE 2

METHODS FOR DEPOSITING POLYMERIC FILMS
ON ELECTRODE SURFACES

dip coating [28]	Electrode is exposed to a dilute solution of polymer. An adsorbed polymer film forms on the electrode surface.
droplet evaporation [29]	Microliter quantities of a dilute solution of a polymer are spreaded and evaporated on the electrode surface.
reductive or oxidative deposition[30]	A polymer is oxidized or reduced electrochemically or photochemically to a less soluble state.
spin coating [31]	A solution of monomer is dropped onto the substrate which is spinning at a high speed.
electro- chemical polymerization [18-24]	A solution of monomer is oxidized or reduced to intermediates which then polymerize rapidly enough to form a film on the electrode surface.
RF plasma polymerization [32]	Vapors of the monomer are exposed to a radio frequency plasma discharge.

The so-called electrochemical polymerization introduces certain polymerizing species directly onto the electrode surface by applying a potential that is high (or low) enough to cause electrooxidation (or electroreduction). This potential can be either a sweep potential offered by cyclic voltammetry or a constant potential. Chemical bonding of the polymer films to the electrode surface is generally unnecessary. Adhesive interactions are sufficient for most purposes.

One of the most important families of redox polymer films is formed by electrooxidative or electroreductive polymerization of complexes of transition metal ions and suitably substituted ligands. These ligands fall into three major categories: 1) pyrrole-substituted complexes; 2) polypyridyl ligands with conjugated olefinic groups, and 3) ligands with primary amino groups on aromatic rings.

a. Pyrrole-substituted complexes

The preparation of modified electrodes by means of electrochemical polymerization of pyrrole and some of its derivatives has been widely developed during the past few years [40]. Thus, pyrrole-based polymers containing redox sites have been prepared by electropolymerization of adequately designed transition metal complexes with pyrrole-substituted ligands. Most of the work that has been performed is summarized in Table 3. A general trend can be

observed: a better film can be obtained with more pyrrole groups in the complex.

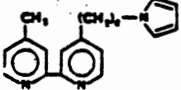
A pyrrole-based cobalt complex film has been used for catalysis of the electroreduction of allyl chloride [45]. The film made by a manganese-porphyrin pyrrole has been applied to the epoxidation of an olefin by molecular oxygen with good rates and faradaic efficiency [43].

Although the polymerization of these pyrrole-substituted complexes has produced interesting polymers aimed at catalyzing certain reactions, these materials do not display, in general, the desired electronic conductivity of polypyrrole. In addition, it appears that steric hindrance and cross-linking effects prevent the growth of the polymer with just one pyrrole group; such is the case with a manganese-porphyrin complex [42,43]. Thus, the copolymerization of the pyrrole-substituted metal complexes with pyrrole has been suggested [50]. This copolymerization has the following advantages: 1) crosslinking effects can be prevented by "dilution" of the macrocyclic complexes in the polymeric backbone, 2) the electronic conductivity can be enhanced, and 3) intermolecular complexation can be provided between the resulting copolymer film chains. Devynck's group [46] attempted this copolymerization and have calculated the stability constants of the complexes in the polymer matrix, which show clearly that the Co(III)-porphyrin sites are complexed by the fixed pyridine polymer.

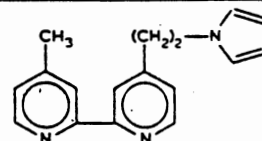
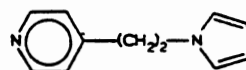
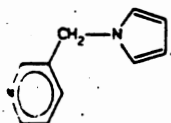
In more recent studies, pyrrole groups have been attached

TABLE 3

 PYRROLE-BASED POLYMER FILMS FORMED
 BY ELECTROPOLYMERIZATION

metal	electrode	media	ligands	reference
Ru	Pt	CH ₃ CN	bipyridine + L ⁽¹⁾	40, 41
Mn	C	CH ₂ Cl ₂ / Bu ₄ NBF ₄	porphyrin-pyrrole pyridine	42, 43
Ni	Pt	CH ₂ Cl ₂ / Bu ₄ NBF ₄	PyTol ₃ P ⁽²⁾ MePy ⁺ Tol ₃ P PlPy ⁺ Tol ₃ P	44
Co	Au	CH ₃ CN/ Et ₄ NClO ₄	4-methyl-4'-(2-pyrrole -1-ylethyl)-2,2'- bipyridine	45
Co	Au	CH ₃ CN/ Et ₄ NClO ₄	pyrrole + porphyrin	45
Cu	Pt Au SnO ₂	CH ₃ CN/ TEAP ⁽³⁾	4-methyl-4'-(2-pyrrole- 1-ylethyl)-2,2'- bipyridine	47, 48
Fe	Pt C Au	CH ₃ CN/ TEAP ⁽³⁾	5-(N-pyrrolylmethyl)- 2,2'-bipyridine	49, 50
Re	Pt			51

(1) L can be:



(2) Py: 4-pyridyl; MePy⁺: 4-(N-Me)-pyridinio
 PlPy⁺: 4-(N-pyrrolyldremethylene)pyridinio
 P: porphyrin

(3) TEAP: Tetra-n-ethylammonium perchlorate

to a range of amine ligands, and the feasibility of electrochemical oxidation of the pyrrole groups to give conducting polymer films has been investigated [24].

Complexes with vinyl-substituted
polypyridyl ligands

Electrode-bound polymer films formed by the reductive polymerization of metal complexes containing either 4-methyl-4'-vinyl-2,2'-bipyridine or 4-vinylpyridine have been studied [52-59]. The ligands form complexes with iron(II), ruthenium(II), and osmium(II), and polymerization can be performed with ligands such as di(4-pyridyl)ethylene, substituted stilbazoles, and N-(4-pyridyl)acrylamides [54]. Polymeric films of these complexes are electroactive, stable, and reasonably uniform. They can be prepared as homopolymer, copolymer, or spatially segregated bilayer coatings.

Murray and co-workers have suggested a "tail-to-tail" radical pair coupling path for the formation of these polymers [53]. A recent study by thin layer chromatography and laser-desorption Fourier transform mass spectrometry demonstrated that normal "polyvinyl-type" chains are formed through chain propagation. For an electrochemically produced poly-Fe(vbpy)₃²⁺ film, an average chain length of seven repeat monomer units has been determined [52].

Complexes with aromatic amino-substituted
ligands

Recent work has introduced a new kind of polymer film formed by oxidative polymerization of transition-metal complexes with an aromatic group or groups on the surrounding ligands [18,20,21,60-62]. The approach of these studies was based on the well known oxidative electropolymerization of aniline and its derivatives [63]. The oxidation of aniline and related compounds to their cation radicals results in a polymeric film growth on electrode surfaces, but polyaniline films prepared by oxidation in pyridine/acetonitrile solution tend to act as electrical insulators [64]. In contrast, films formed by the corresponding complexes with transition metals display well defined electrochemical activity and continued film growth via film-mediated oxidation of additional monomers.

Murray et al. [21] have performed some extensive research on the subject. They first found that polypyridyl complexes of ruthenium-containing aromatic amino groups, such as {[4-aminopyridine]₂[2,2'-bipyridine]₂ Ru}²⁺; {[3-aminopyridine]₂[2,2'-bipyridine]₂ Ru}²⁺; {[5-amino-1,10-phenanthroline]₂[2,2'-bipyridine] Ru}²⁺, undergo electrochemically induced oxidative polymerization reactions. The resulting polymers are fairly stable and electrochemically active on the electrode surface which can be Pt, SnO₂, or vitreous carbon. Complexes containing only

one amino group are difficult to polymerize but can be copolymerized with {[5-amino-1,10-phenanthroline]₃Ru}²⁺. Since then, complexes of iron(II) and cobalt(II) with similar ligands have been electropolymerized on several electrode surfaces such as gold and glassy carbon [18,20,60-62]. Both anodic and cathodic polymerization have been used.

Ellis et al. [21] have proposed a mechanism for the [5-amino-1,10-phenanthroline-metal] oxidative polymerization. The first step involves a ligand-based oxidation to give a cation radical. Further oxidation of a resulting imine-linked dimer with C-N coupling leads to sustained polymerization. The reductive polymerization of the amino-substituted phenanthroline bipyridine complexes can be explained by the reduction of the bipyridine rings [28]. The first step involves a ligand-based reduction to give an anion radical that allows a C-N coupling. Further reduction can lead to further polymerization.

Electrochemical Properties of Redox

Film-coated Electrodes

There has been sustained interest in the electrochemical properties of the redox polymer-modified electrodes. In order to reach a better understanding of the fundamental nature of the polymer film on the electrode surface, Inzelt [78] introduced a model for polymer film electrodes consistent with the results obtained by electrochemical and other techniques:

1. The multilayer polymer film coated on the electrode surface is a swollen polyelectrolyte gel, the originally neutral polymer is transformed into a polyelectrolyte as a function of the potential.

2. The coatings are permeable to solvent molecules and ions. The sorption of counterions is a necessary process coupled to electron transfer to maintain electroneutrality, if there are no follow-up chemical reactions. Motion of counterions should also be taken into account.

3. As a consequence of incorporation of ions and solvent molecules into the film, swelling or shrinkage of the polymer matrix may take place.

4. Polyelectrolytes are most sensitive to structure and environment. A small difference in the interaction may have a great influence on the properties of the polyelectrolytes.

5. According to present thinking on the mechanism of charge transport, the redox centers in an electrochemically active polymer film become oxidized or reduced by a succession of electron transfer self-exchange reactions between neighboring sites (recall Fig. 2). This electron site-site hopping which resembles a diffusion process has been shown by several groups [65-67]. As discussed earlier, this diffusion process is proportional to a charge diffusion constant D_{ct} . A great variety of D_{ct} values have been calculated. Inzelt et al. [68] have shown that, in several cases, reliable charge transport coefficients can be

extracted from the experimental $i-t^{-1/2}$ data in potential-step chronoamperometry with the help of computer simulation.

The electron transport rate can be controlled by:

1. The electron-hopping across the polymer film.
2. The movement of counterions to achieve electrical neutrality.
3. The intrinsic thermal barrier to electron transfer.

In different materials, the rate-determining step may be different and it is conceivable that it might be altered in a given polymer material by systematic change of some parameters such as the concentration of electroactive sites in the polymer.

Studies of the dependency of D_{ct} on the electroactive site concentration have been conducted [79,80]. These investigations were aimed at identifying the rate-determining step in the overall charge transport process. Some diffusional tailing and larger peak separation in cyclic voltammograms were observed when the concentration of redox sites was low; this indicated a slower electron transport rather than a more concentrated redox site in polymer.

Electron transport dynamics were studied by Faulkners et al. [69,70] for the $Fe(CN)_6^{3-/4-}$ in partially quaternized poly(vinylpyridine)-modified electrodes. They tried to identify the major factors controlling electron diffusion in the electroactive films. Variable-temperature chronocoulometry was employed to measure the electron diffusion coefficients (D_e) and the activation energies (E_a)

for electron transport. The results suggest that counter-ion motion is not a factor limiting the electron motion. The polymer lattice clearly becomes more crosslinked upon taking up redox ions. This effect induces a loss in short-range ion mobility within the film and causes a decline in D_e as the film is more heavily loaded. The anion dependence of E_a is explained on the basis of changes in internal structure reflecting interactions within the cationic polymer lattice. The same authors have also found that perchlorate ions produce nearly dehydrated, difficultly permeable films. In another study, a similar conclusion has been drawn for perchlorate [71].

The effect of chemical environment (solvent and nature and concentration of the supporting electrolyte) and temperature on the electrochemistry of polymer films on electrodes has also been investigated [72,73].

The configuration of the polymer chains in solution and/or the swelling of polymer gels are determined by the interaction between the polymer segments and the solvent molecules. This solvent effect can be observed in changes of D_{ct} values, the shapes of cyclic voltammetry waves and other results. Up to now there has been no simple explanation of these observations because of the interrelationship of solvent effect and charge-compensating counterion effect.

In regard to the nature of the electrolyte, two effects should be considered. First, an increase in the size of counterions may lead to a decreased mobility in the film.

Second, polyvalent ions may enhance the formation of cross-links between chains and thus produce a more compact structure for the electrolyzed film. This picture may be further complicated by the influence of solvation of ions and other specific interactions. Parallel to the studies carried out on the effect of the nature of counterions, investigations on the effect of the concentration of counterions were also underway [72, 73]. An increased stability and a more compact structure of the film are to be expected in concentrated solutions. In this case the concentration of the redox site is high, so that an increase in the rate of electron hopping is expected.

Conclusions

In general, research on modified electrodes, especially polymer-coated modified electrodes, have been a very active and fruitful area. After the very wide search on the possibility of forming varied kinds of polymeric films on the electrode surfaces, researchers began to study the mechanism of polymerization as well as the charge transport across the film. Since each polymer film-coated electrode has its unique properties and also so many factors are involved, it has been very difficult to get a general picture, although some very specific explanations on electron transport dynamics of polymer-film-coated electrode have been offered. Meanwhile, the research on practical applications of polymer-film-coated electrodes is still a rather unexplored area.

Considerable work needs to be done in the area of electron transport dynamics, which involves the function of counterion and solvation of the polymer matrix as well as other phenomena. It is also necessary to search for new directions of practical application.

CHAPTER III

ELECTROOXIDATIVE POLYMERIZATION OF TRIS[5-AMINO-1-10-PHENANTHROLINE]- IRON(II) ON GLASSY CARBON

Experimental

Apparatus

Cyclic voltammetric measurements were carried out with a BAS-100 electrochemical analyzer (Bioanalytical Systems, West Lafayette, IN).

The glassy carbon electrode used was 1.5 mm in radius and also obtained from Bioanalytical Systems. A clean electrode was prepared by polishing the glassy carbon surface successively with 0.50- μm and 1.0 μm α -alumina (Bioanalytical Systems) on an optically flat plate, each for 30 s. After polishing, the electrode was cleaned in an ultrasonic bath with deionized-distilled water for 1 min.

A Ag/AgCl, 3 M KCl electrode was used as reference electrode and a Pt wire served as auxiliary electrode.

Reagents and Solutions

All reagents used were of analytical reagent grade. Deionized-distilled water was used for preparation of all

aqueous solutions. Acetonitrile (Fisher Scientific, Fair Lawn, NJ) was stored over 0.4-nm molecular sieves (Linde Division, Union Carbide, Danbury, CT). The 5-amino-1,10-phenanthroline was obtained from Polysciences (Warrington, PA) and was used as received. Ferrous chloride (Fisher Scientific) was dried at 100°C for 24 h before use. Sodium perchlorate (anhydrous) was obtained from GFS Chemicals (Columbus, OH).

Tris[5-amino-1,10-phenanthroline]iron[III] Complex Solution The stock solution used was 3 mM in complex concentration. It was obtained by dissolving 5% excess of ligand with ferrous chloride in acetonitrile. A small amount of concentrated acetic acid (5 ml/100 ml solution) was added to help the solubilization process.

Supporting Electrolyte The supporting electrolyte used was 0.10 M sodium perchlorate in acetonitrile.

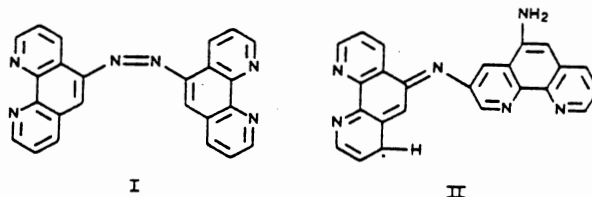
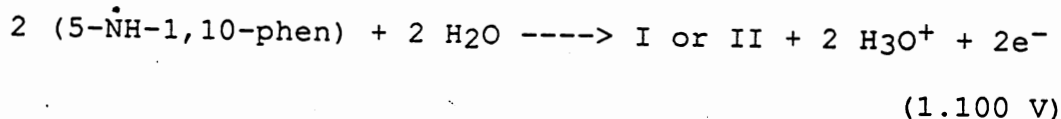
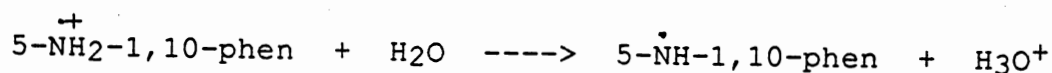
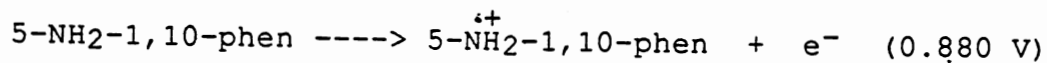
Results and Discussion

Electrochemical Behavior of 5-amino-1,10-phenanthroline

In the cyclic voltammogram of 5-amino-1,10-phenanthroline solution, irreversible oxidation waves appeared at 0.880 and 1.100 V as well as a reduction peak at 0.500 V. Peak currents at 0.880 and 1.100 V decreased in successive cycles while those around 0.500 V increased. After a certain number

of cycles, the 5-amino-1,10-phenanthroline was found immobilized on the electrode surface.

1,10-Phenanthroline does not show electrochemical reactivity in the 0.700 to 1.200 V range which indicates that oxidations at 0.800 and 1.100 V involve the amino group. The mechanism of electrooxidation of aromatic amines is well documented in the literature [63]. Such oxidations involve: (a) removal of one electron from the lone pair of electrons on the amine nitrogen, (b) loss of a proton from the amine, and (c) coupling of the units. When applied to 5-amino-1,10-phenanthroline, we have:



Electrooxidative Polymerization of Tris[5-amino-1,10-phenanthroline]iron[II]

Figure 3 shows a cyclic voltammogram at a glassy-carbon electrode of an acetonitrile solution 0.030 mM in tris[5-amino-1,10-phenanthroline]iron[II] complex and 0.10 M in NaClO₄. At the first cycle, similar amine oxidation peaks (0.880 and 1.100 V) are seen but the peaks due to amine oxidation disappear and a pair of symmetric anodic and cathodic peaks appeared at 1.000 V, these are due to reaction of the central metal ion immobilized on the glassy-carbon surface. An increase in these peak currents can be clearly seen after each successive cycle. When the electrode surface was washed and then placed in a blank electrolyte solution (acetonitrile), the electrochemical behavior of the central metal ion was unchanged. With repeated cycles, the reduction and oxidation peaks still remained the same (see Figure 4). This indicated that the polymer film on the glassy-carbon was stable.

The first polymerization cycles showed that peak currents are proportional to the cycle number (Figure 5). The rate of peak current growth was also found to be proportional to the original concentration of complex in the solution. Concentrations of 0.30 and 1.00 mM, for example, gave reduction current increases of 2.3 and 7.2 $\mu\text{A}/\text{cycle}$, respectively.

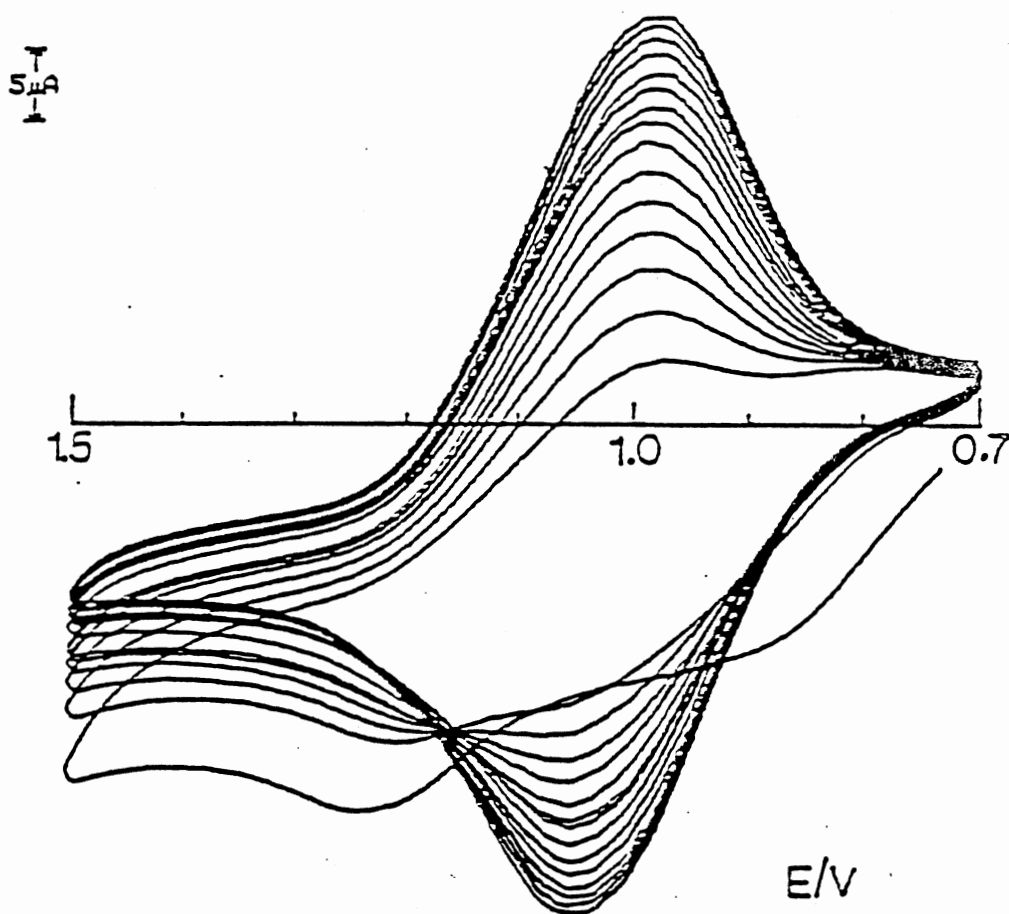


Figure 3. Repeated Cyclic Voltammograms of a 0.030 mM Solution of Tris-[5-amino-1,10-phenanthroline]Fe(II) in Acetonitrile at a Glassy-Carbon Electrode. Supporting Electrolyte: 0.1 M NaClO₄ Scan Rate 50 mV s⁻¹

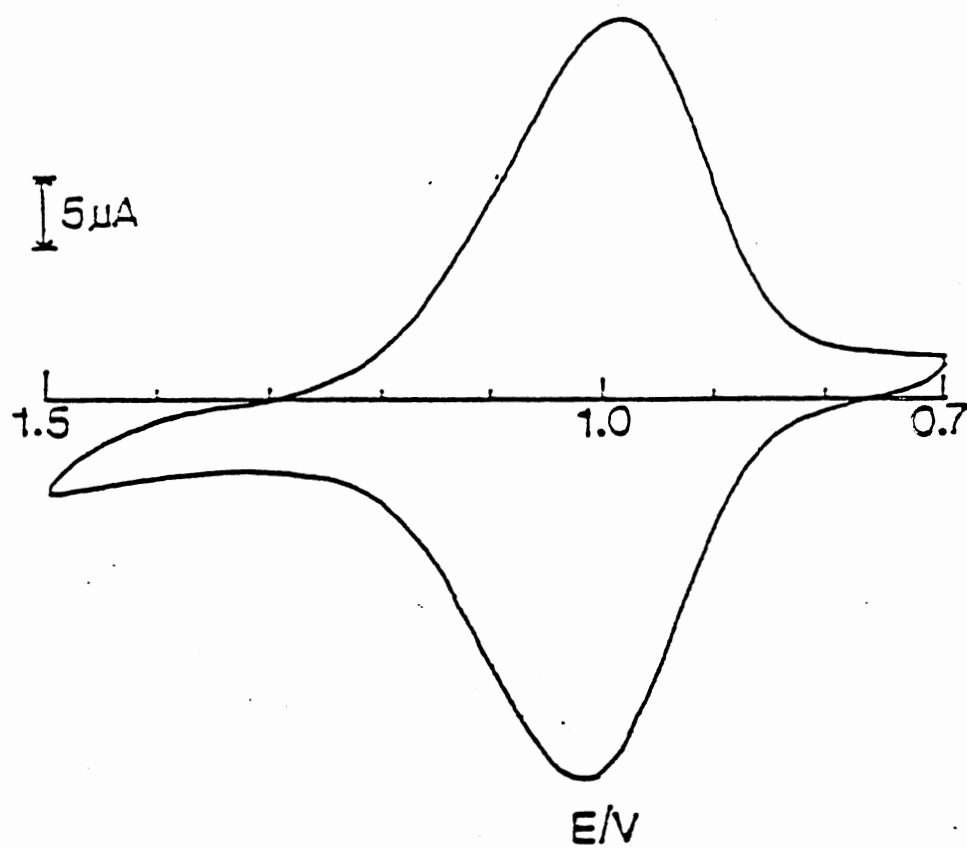


Figure 4. Cyclic Voltammograms Obtained with a Polymer-coated Electrode in 0.10 M NaClO₄. Scan Rate 50 mV s⁻¹

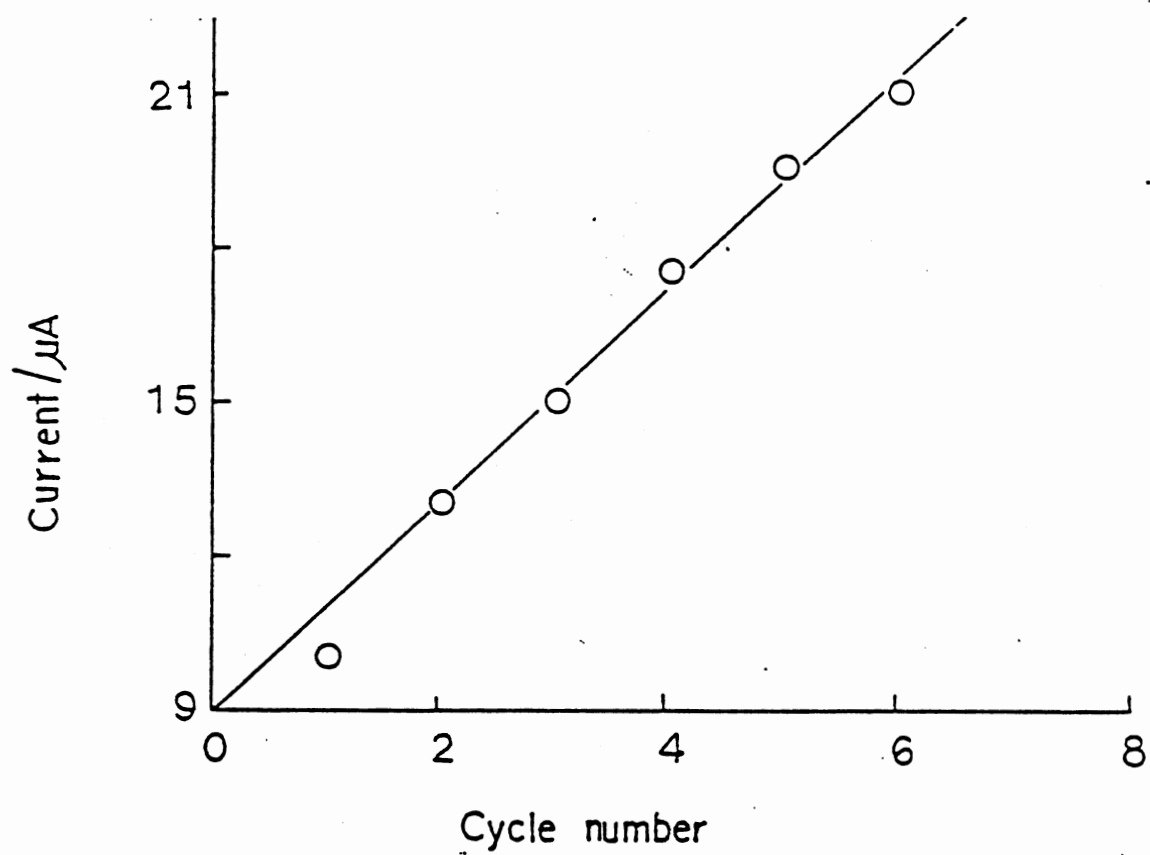


Figure 5. Reduction Peak Currents as a Function of Cycle Number for Data in Figure 3

Effect of Scanning Rate on the Cyclic Voltammogram
Obtained with the Polymer-film-coated
Glassy-carbon Electrode

The effect of scanning rate on the response of the modified electrode in cyclic voltammetry was investigated. This is a reliable and simple way to get useful information about charge transport inside the polymer film. Usually a linear plot between the square root of scanning rate and current indicates a diffusion-controlled charge transport and the charge diffusion coefficient can be calculated from the slope. The relationship between the square root of the scanning rate and the peak height is plotted in Figure 6. A linear relationship was in fact obtained, indicating the charge transport across the polymer film is a diffusion-controlled process.

For a reversible diffusion-controlled process:

$$i_p = 2.69 \times 10^5 \ n^{3/2} \ A \ D_0^{1/2} \ V^{1/2} \ C_0$$

where i_p is peak current; n gives the number of electron transfers involved in the process; A is the area of the electrode surface; D_0 is the charge diffusion coefficient; V is the potential scanning rate; and C_0 is the concentration of the active redox site.

This is valid at 25 °C, for A in cm^2 , D_0 in cm^2/sec , C_0 in mol/cm^3 , V in V/sec . and i_p in amperes.

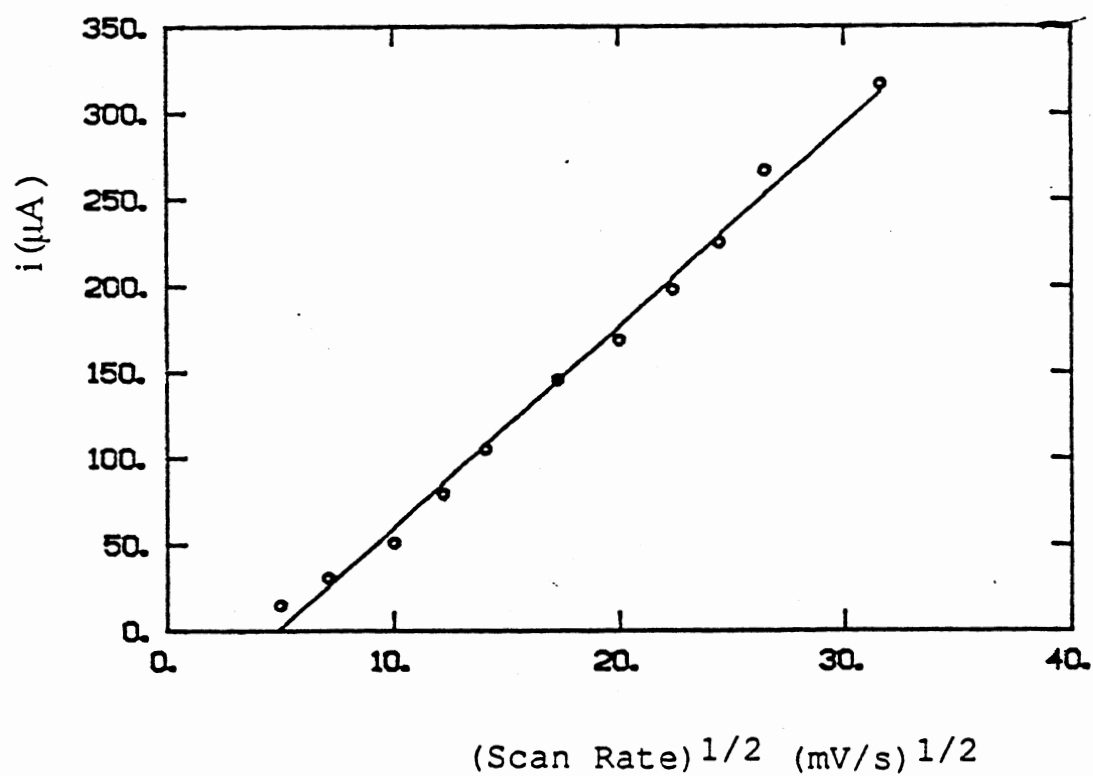


Figure 6. Peak Current vs Square Root of Scan Rate Plot. in Cyclic Voltammograms of a Polymer-modified Electrode in 0.10 M KClO_4

According to the estimation from Nayasulu and Mottola [18], in a freshly prepared tris[5-amino-1,10-phenanthroline]Fe[II] polymer-film-coated electrode surface:

$$\underline{C}_O = 7.3 \times 10^{-4} \text{ mol/cm}^3$$

for

$$\underline{A} = 0.71 \text{ cm}^2$$

From the linear plot of $\underline{V}^{1/2}$ vs i in Figure 6, the slope obtained is:

$$\text{slope} = 11.9 \text{ A/(mV/s)}^{1/2}$$

All these values are substituted back into the above equation to obtain the charge transport diffusion coefficient \underline{D}_O : $7.1 \times 10^{-10} \text{ cm}^2\text{s}^{-1}$.

The plot of the difference in two peak potentials versus the square root of the scanning rate is presented in Figure 7. As the potential scanning rate increases, a bigger separation in peak potential is observed. This indicates that a less reversible electrochemical process was occurring.

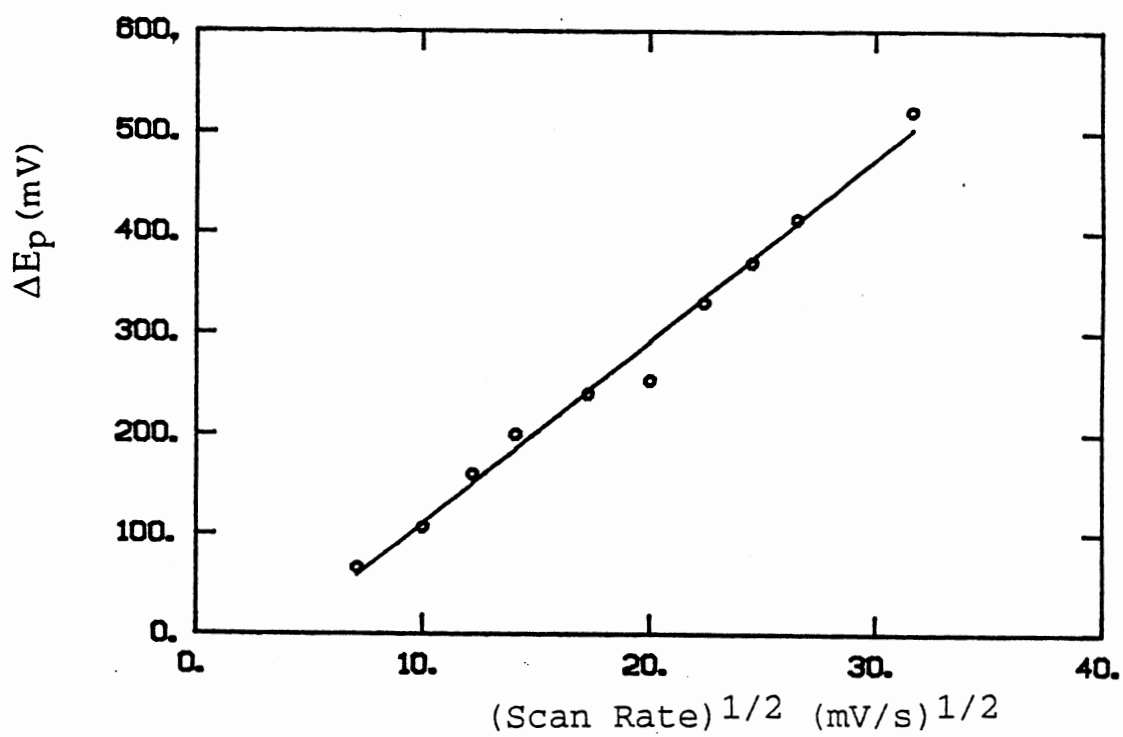


Figure 7. Difference in Two Peak Potentials
(E_{pa}-E_{pc}) vs Square Root of Scan Rate
Plot in Cyclic Voltammograms of a
Polymer-modified Electrode in 0.10 M
KClO₄

CHAPTER IV

SOME BASIC PROPERTIES OF TRIS[5-AMINO-1-10- PHENANTHROLINE]IRON(II) POLYMERIC FILMS ON GLASSY CARBON

Experimental

Apparatus

Cyclic voltammetric measurements were carried out with a BAS-100 electrochemical analyzer (Bioanalytical Systems, West Lafayette, IN).

Electron scanning micrographs were taken with a Cambridge Stereoscan 250 Mark II with a Traco Northern TN 5500 x-ray attachment. A DMS 200 UV visible spectrophotometer (Varian Instrument Group, Australia) was used for the collection of UV-visible spectral information. All the infrared spectra were obtained with a Perkin Elmer 681 infrared spectrophotometer.

The glassy-carbon electrode used was treated as described in Chapter 3. The wax-graphite electrode used (3 mm in radius) was composed of 40% paraffin wax and 60% graphite. The required amount of wax (W. & F. Mfg Co., Inc., Buffalo, NY) was melted in a 50-ml beaker; then the required amount of graphite (Ultra Carbon, Bay City, MI) was added to the wax.

The suspension was mixed well and loaded into the electrode well while the wax was still in the liquid form. The electrode was polished on a piece of clean card before using. A Ag/AgCl, 3 M KCl electrode was used as reference electrode and a Pt wire served as auxiliary electrode.

Procedures

Polymerization on Glassy-carbon or Carbon Wax Paste

Electrodes A well polished glassy-carbon electrode, along with the reference and auxiliary electrodes, were dipped into a solution containing 0.20 mM complex and 0.10 M sodium perchlorate in acetonitrile. Cyclic voltammetry was performed for a given number of cycles over a potential range of 0.0 V to 2.0 V. The scanning rate used was 50 mV per second. A shining blue polymer film could be seen over the electrode surface. This polymer-film-coated electrode was rinsed with deionized water and kept stored in supporting electrolyte for further investigation.

UV-Visible Spectra Three types of solutions were used to obtain the spectra in order to see the difference in structure before and after polymerization. These three solutions were:

Polymer solution: The polymer on the electrode surface was dissolved directly into N,N-dimethylformamide. The resulting solution was further diluted with the same solvent until a suitable absorbance reading was obtained.

Complex solution: The original stock complex solution was evaporated until a precipitate of the complex was obtained. This precipitate was dissolved in N,N-dimethylformamide to reach a concentration for which the absorbance was about 1.0.

Ligand solution: 5-Amino-1,10-phenanthroline was directly used to make the solution. The solvent used was again N,N-dimethylformamide. The concentration was adjusted as previously mentioned.

Infrared spectra The polymer sample was obtained by dissolving the polymer film into N,N-dimethylformamide, then allowing the solution to evaporate under vacuum for two days and incorporating the residue into a KBr pellet. The sample of the complex was obtained by evaporating the complex solution prior to making the KBr pellet. All chemicals used here were dried under vacuum for two days.

Electron scanning micrographs The blank electrode used here was a carbon-wax paste electrode for the convenience of fitting into the instrument.. The polymer-film-coated electrode was prepared as described earlier and performing 250 cycles.

Results and Discussion

Electron Scanning Micrograph

A freshly made polymer-coated wax-paste electrode (as described in procedure) and a plain wax-paste electrode were used to obtain the electron scanning micrographs. These gave proof of the presence of a polymer film on the surface (see Figures 8 and 9). The uncovered surface was rather rough but the surface after polymerization was considerably smoother. Figure 10 identifies two of the elements existing on the surface as iron and chloride. Chloride is from the electrostatically held counterion in the film.

UV-visible Spectra

The UV-visible spectra of polymer/DMF solution, original complex/DMF solution, and ligand/DMF solution are presented in Figures 11, 12, 13, and 14. In the case of the complex, two differently prepared solutions were used: one by direct evaporation of the stock solution and the other by dissolving the precipitate produced by ammonium hexafluorophosphate from stock solution of the complex. No distinguishable difference between samples prepared in these two ways was observed. The major absorbance peaks from the corresponding spectra are listed in Table 4.

In Table 4, the two similar values for absorption peak 4 are due to the electron transition of the central metal iron

TABLE 4

ABSORPTION WAVELENGTH FOR PEAKS
IN THE UV-VIS REGION

wavelength (nm)	1	2	3	4
polymer,	294.8	340.0	386.9	528.5
complex,	274.3	288.2	368.1	527.1
ligand,	275.0	281.6	343.3	

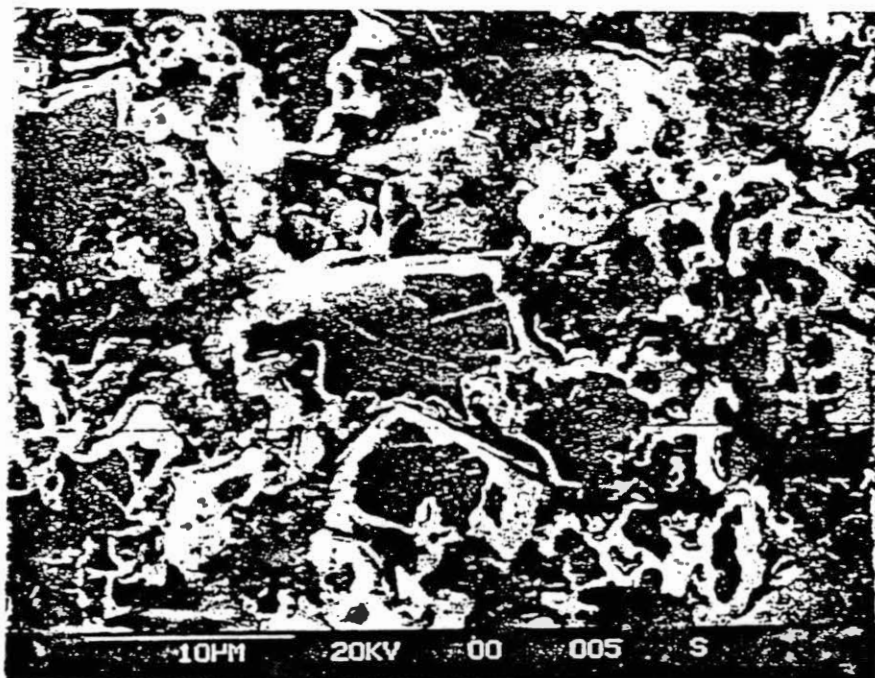


Figure 8. Scanning Electron Micrograph of a Naked Wax-carbon Paste Electrode

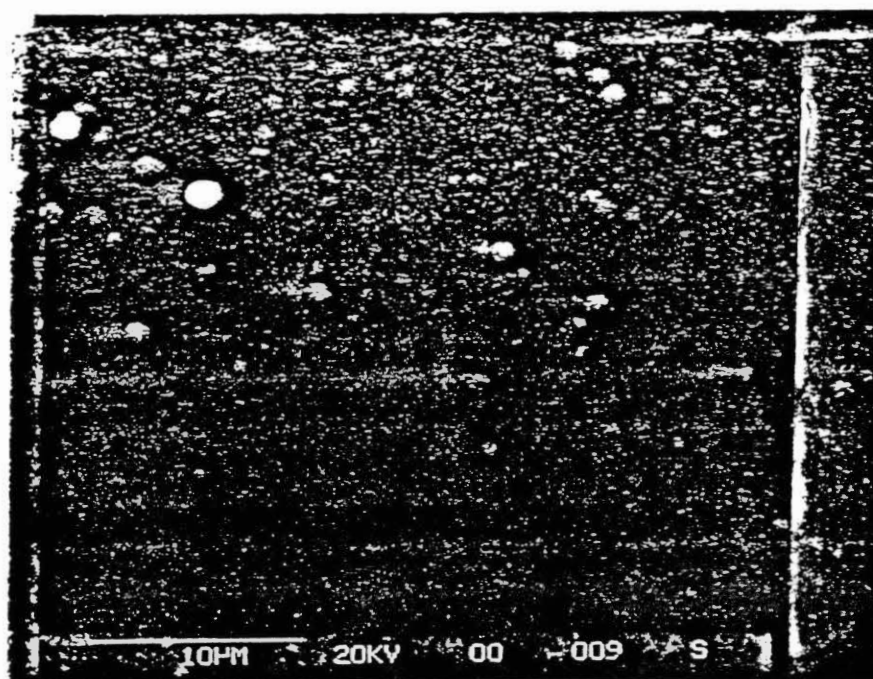


Figure 9. Scanning Electron Micrograph of a Polymer-coated Wax-carbon Paste Electrode. The Polymer Was Made by Electrolysis at a Potential of 1.500 V for 2 Hours (for thicker film).

Cursor: 0.100keV = 0

ROI (1) 0.000: 0.000

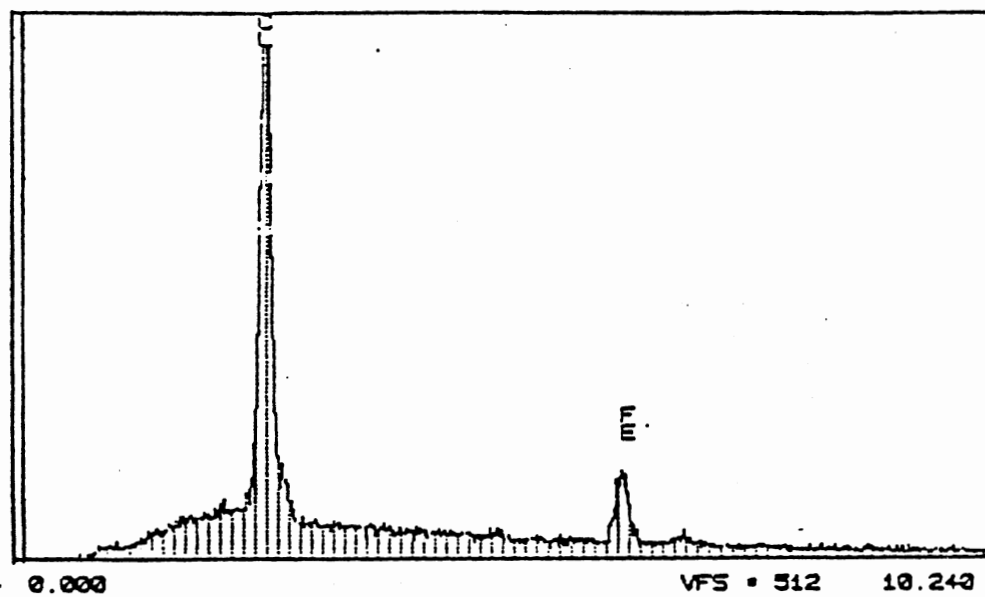


Figure 10 X-ray Deffraction Pattern of a
Polymer-coated Wax-carbon paste
Electrode.

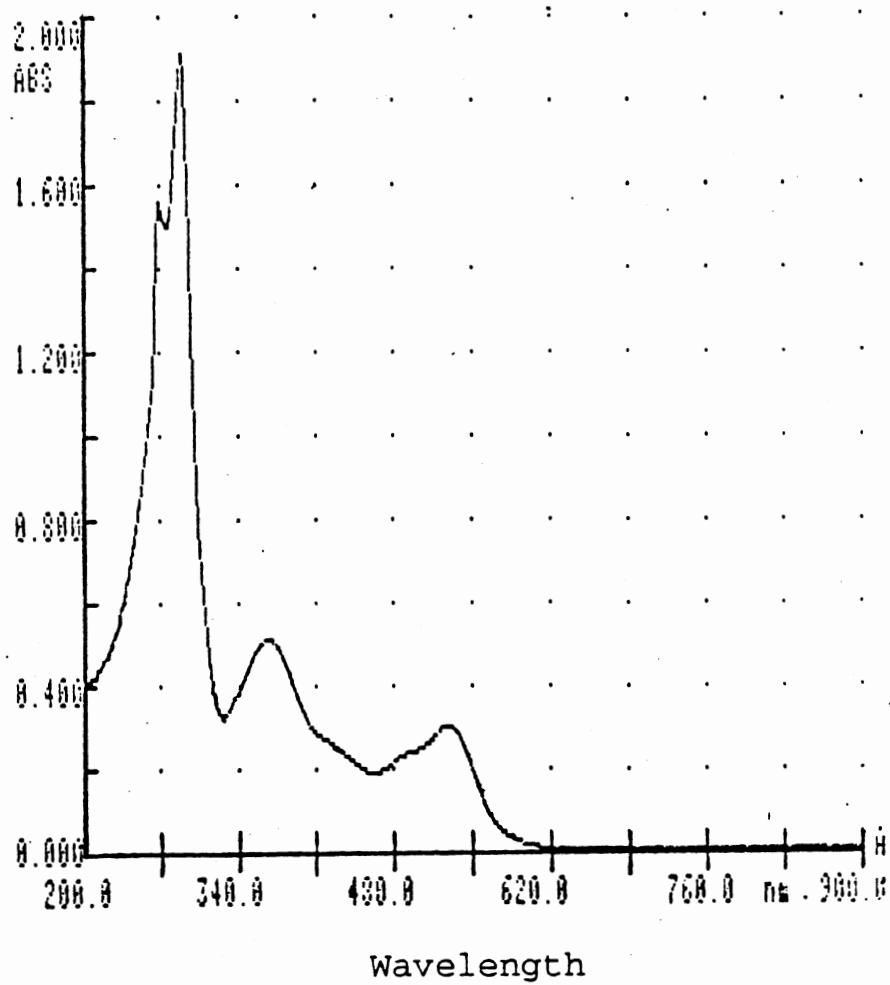


Figure 11. UV-visible Absorption Spectrum of Polymer/DMF Solution.

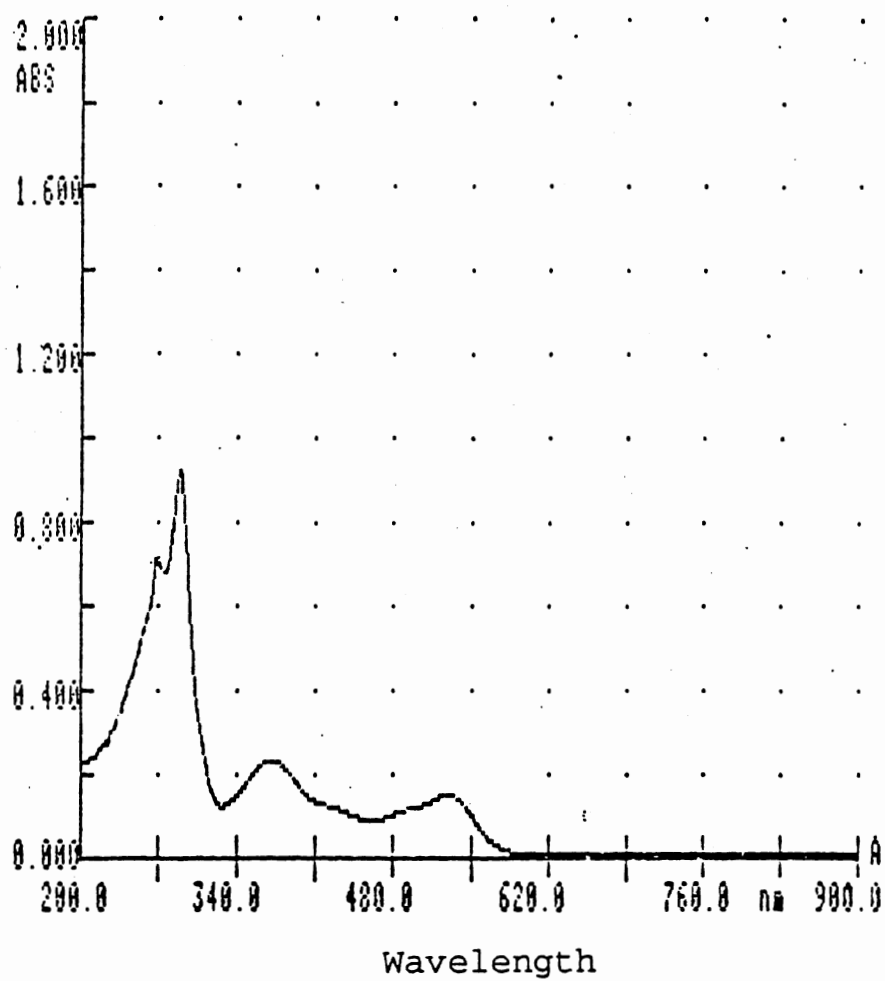


Figure 12. UV-visible Absorption Spectrum of Complex/DMF Solution.

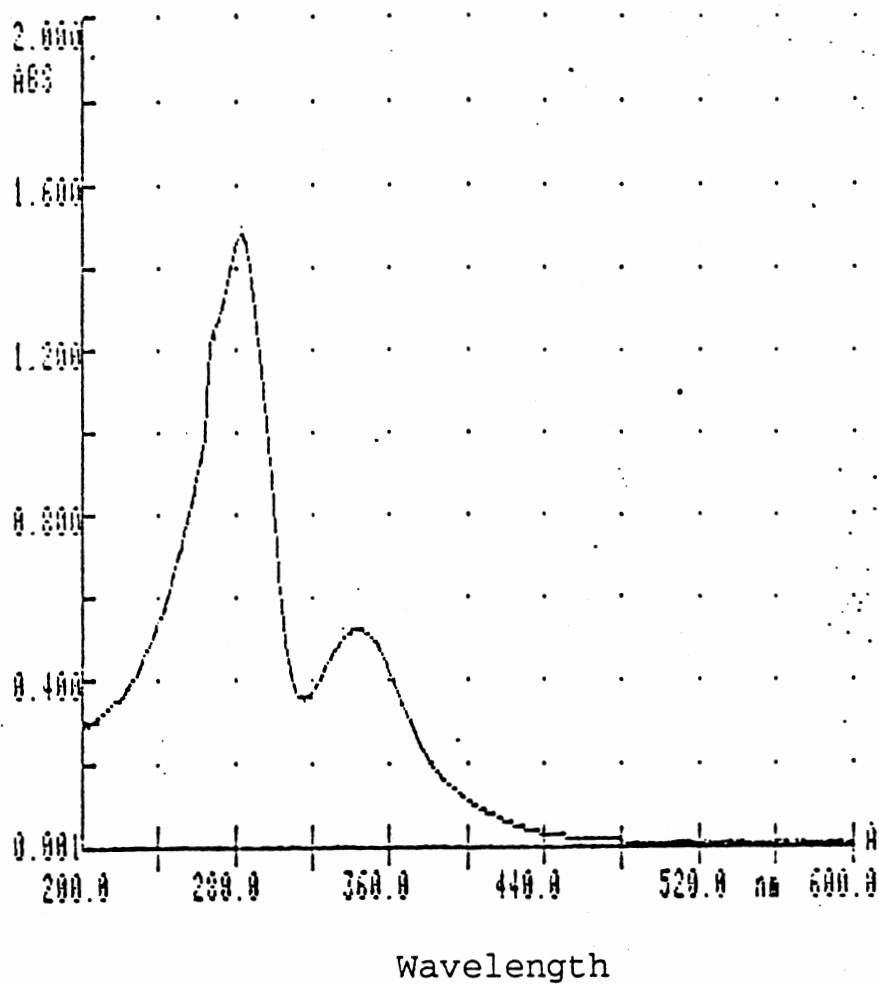


Figure 13 UV-visible Absorption Spectrum of
Precipitate/DMF
Solution.

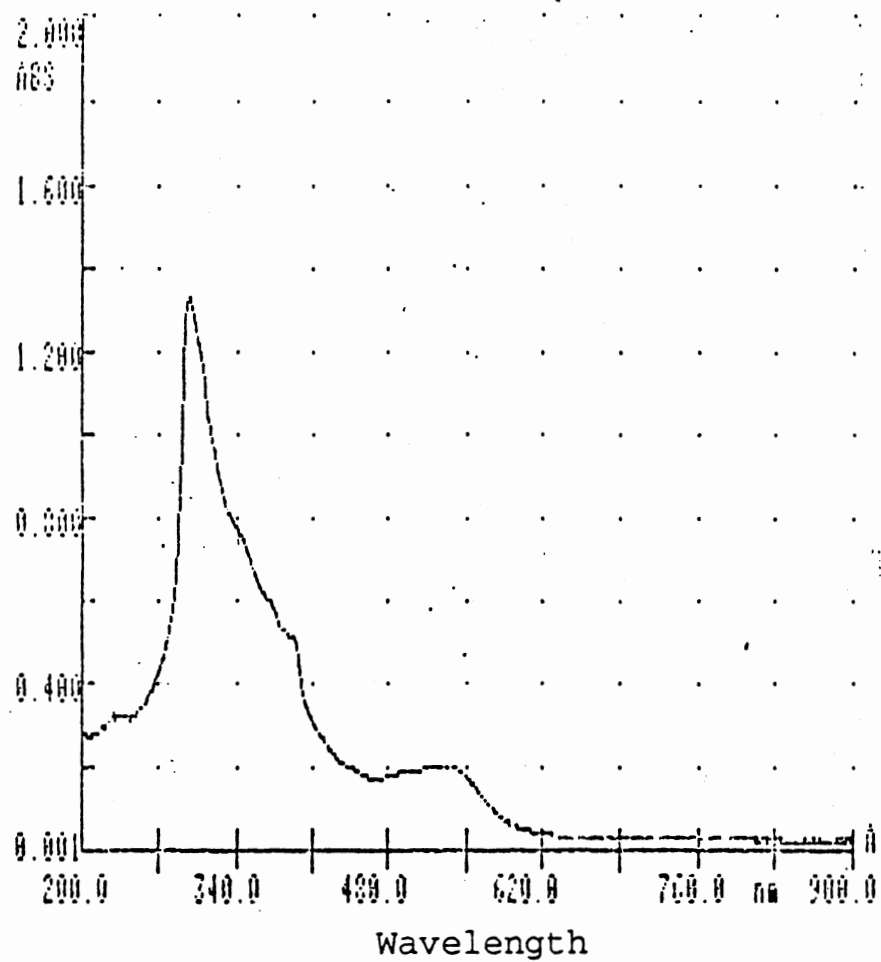


Figure 14. UV-visible Absorption Spectrum of 5-amino-1,10-phenanthroline/DMF Solution.

in the complex. Peak 1 is caused by the π - π electron transition while the n - π electron transitions induced the absorption at peak 2 and peak 3. Two absorption peaks are caused by n - π electron transitions because two types of lone pair of electrons exist in the system. A red shift occurs in the polymer absorption and gives an indication of a more conjugated structure (most likely a more extended conjugation) in the polymer.

Infrared spectra

Two clear changes were observed (Figures 14 and 15) between the infrared spectrum for the complex and that of the polymer. These differences are:

- 1) A strong triplet peak at about 1100 cm^{-1} (1080, 1110, and 1140) in the spectrum of the polymer, whereas the spectrum of the complex has only a broad weak absorption over this region.

- 2) The peak appearing at 850 cm^{-1} in the spectrum of the original complex does not appear in the spectrum of the polymer.

In the spectrum of the complex, the 850 cm^{-1} peak can be assigned to the N-H wag, but in the spectrum of the polymer, there is no corresponding absorption peak. This is an indication that all N-H bonds were broken in the polymerization reaction.

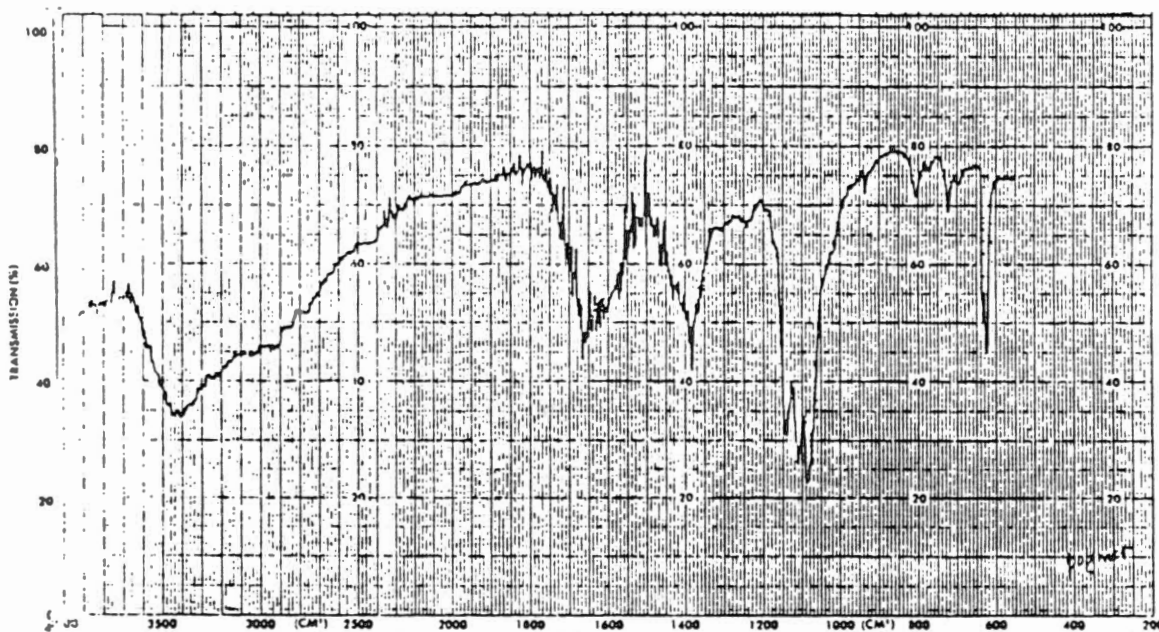


Figure 15. Infrared Spectrum of Polymer in KBr.

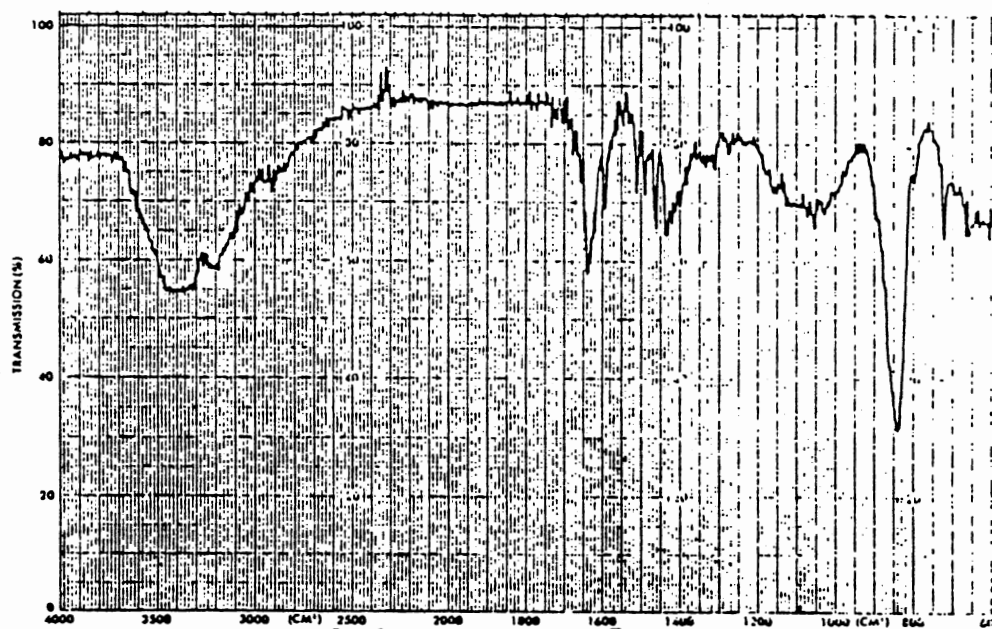


Figure 16. Infrared Spectrum of Complex in KBr.

The only possible explanation for the 1100 cm^{-1} peak is the C-N stretching. The big increase in intensity could be an indication of the formation of new C-N bonds. So compare the two possible structures listed in page 30, it is determined that structure II is the repeating unit of the polymer of tris[5-amino-1,10-phenanthroline]Fe[II].

CHAPTER V

EFFECT OF COUNTERIONS IN TRIS[5-AMINO-1,10-PHENANTHROLINE]IRON[II]-POLYMER-FILM-COATED GLASSY-CARBON ELECTRODES.

Experimental

Reagents and Solutions

Solution of iron complex. A 0.50 mM tris[5-amino-1,10-phenanthroline]iron[II] solution in acetonitrile 0.10 M in NaClO₄ was used for polymer preparation.

Supporting electrolyte solution. All chemicals used as supporting electrolyte were of reagent grade. The concentration of supporting electrolyte solutions was 0.10 M.

Procedures

Film preparation. A well polished glassy-carbon electrode was dipped into the solution of iron complex along with a reference electrode (Ag/AgCl, 3 M KCl) and an auxiliary electrode (Pt). Electrooxidative polymerization was performed by application of cyclic voltammetry as described earlier. The scan rate was set at 50 mV per second in the range from 0 to 2.00 V. Thirty cycles were used for preparation of each film.

Cyclic voltammetry The polymer-covered surface was washed first with acetonitrile and then with water. After this washing, the background current was recorded by cyclic voltammetry in the original blank solution (0.10 M sodium perchlorate in acetonitrile). The cyclic voltammetric experiments were then performed in aqueous solutions of different supporting electrolytes.

Effects in NO₂ Detection. This part of the work was performed with a continuous-flow system. Different supporting electrolytes were used as carrier solution in order to obtain the response in the presence of different counterions.

Experimental parameters:

Concentration of NO₂: 12 ppb (v/v)
Applied voltage: 1.000 V vs Ag/AgCl, 3M KCl.
Injected volume: 0.20 ml
Sample size: 200 nl
Carrier flow rate: 6 ml/min.

Results and Discussion

Cyclic Voltammetry

As was mentioned in Chapter 3, the electron motion in and out of the film can be controlled by one or more of the following factors:

1. Electron hopping between redox centers inside the polymeric film.
2. Counterion diffusion into and out of the film to effect charge compensation.
3. Diffusion of counterions from the bulk of the solution towards the electrode surface.

Compared to counterion diffusion inside the polymer film, diffusion in the solution could not be the rate-limiting factor because of the more compact structure of the polymer matrix. Table 5 lists all the peak currents from cyclic voltammograms obtained in different supporting electrolyte solutions. From Table 5, we see that peak currents change significantly when the type of counterion is changed. Consequently, it is not possible for electron hopping in the film alone to be the controlling factor. Such a possibility, however, cannot be ruled out because the change in current might also be caused by a change of rate of electron hopping between redox centers, and this change in rate might be due to the specific interactions between the polymeric matrix and the different counterions. There is another possible controlling factor -- the motion of the counterion inside the polymer film. Finally, solvation could also contribute somewhat to a decrease in current; this is discussed below.

According to the shape and size as well as the voltammetric response in the presence of different counterions, there fall into three groups:

TABLE 5

HYDRATION RATE, POTENTIAL SHIFTS, PEAK CURRENTS^a
 FROM CYCLIC VOLTAMMOGRAMS AND NO₂(g) INJECTIONS
 IN DIFFERENT SUPPORTING ELECTROLYTE SOLUTIONS

Counter Anion	Ionic Mobility (ohm ⁻¹ cm ²)	Hydration Rate (nA/s)	ΔE (V)	Anodic Peak Current ^a in CV	current in NO ₂ (g) inj. (nA)
F ⁻	46.7	3.13	-0.03	0.85	0.85
Cl ⁻	65.4	2.27	0.04	1.00	1.00
NO ₃ ⁻	61.7	1.11	/	0.84	1.20
ClO ₃ ⁻	55.0	1.23	-0.02	0.77	0.96
BrO ₃ ⁻	47.9	1.42	0.04	0.80	1.06
ClO ₄ ⁻	56.0	0.58	/	0.60	0.75
HCOO ⁻	47.0	1.68	-0.12	0.84	1.16
CH ₃ COO ⁻	35.0	1.95	-0.13	0.46	1.06
CCl ₃ COO ⁻	38.0 ^b	/	-0.02	0.85	0.85
C ₆ H ₃ N ₃ O ₇ ⁻	25.4	0.11	/	0.74	0.42
C ₆ H ₅ COO ⁻	27.9 ^b	/	-0.09	0.39	0.56

- a. All the current values listed in the table are normalized to the response in presence of Cl⁻.
 b. Estimated value.

1. Simple ions, such as F^- and Cl^- . The higher the ionic mobility in water, the higher the response.
2. NO_3^- , ClO_3^- , and BrO_3^- . Their ionic mobilities range from 1.915 to 1.49, but the responses are more or less the same.
3. Anions of organic acids. Except for picrate, the response decreases with the decreasing of ionic mobility.

The Hydration Process

The extent of solvation is a very important factor in determining the rate of electron transport because of its effects on the internal structure of the polymer film, such as rigidity and compactness.

The peak currents in cyclic voltammetry of the polymer film-coated electrode decreased cycle by cycle when the electrode was dipped into an aqueous supporting electrolyte solution. This decrease in current is due to solvation. Hence, by calculating the rate of decrease of current, a relative rate of hydration can be obtained (data listed in Table 5).

$$\text{Rate} = \Delta i / \Delta t,$$

where Δi is the difference of peak current between the first and the second cycle, Δt is the time needed for the scanning of one cycle. This rate has units of nA / s.

The rate of peak current decrease varies greatly in the different counterion solutions. The most plausible reason for the current decrease is the swelling of the polymer film due to hydration. A very fast decrease in peak current is seen with counterion solutions such as those of HCOO^- , Cl^- , and F^- ; this means that the solvation process is completed very rapidly. These examples are shown in Figure 17. The slowest hydration occurs in the solution of the very bulky picrate anion (see Figure 18). And a rather mild solvation takes place in perchlorate solution (see Figure 19), in which we can actually see the solvation step by step in the cyclic voltammograms.

Two other interesting phenomena can be seen from the cyclic voltammograms:

(1) The reduction peaks decrease in magnitude much faster than the oxidation peaks in all solutions except that of picrate. It can be summarized that the larger amount of water inside the polymer is due to hydration and this must lead to a larger effective separation between the redox ($\text{Fe[II]}/\text{Fe[III]}$) centers. In such a case, the electron hopping between those redox centers becomes more sluggish. Apparently, the effects of hydration on the rates of electron hopping in different directions are not the same: the rate of electron hopping in the direction of oxidation suffers considerably less from hydration than that in the direction of reduction. From all this discussion it can be concluded .

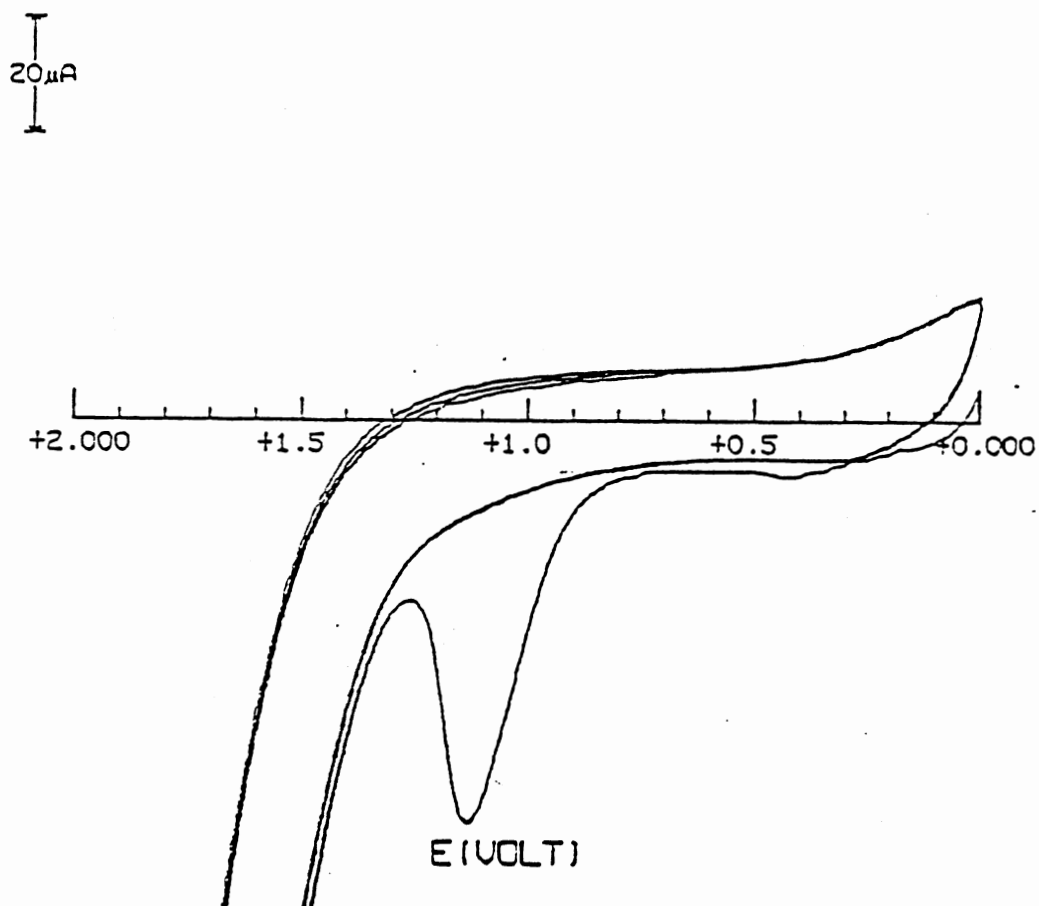


Figure 17. Cyclic Voltammograms of Film-coated Electrode in 0.10 M HCOO⁻ Aqueous Solution.

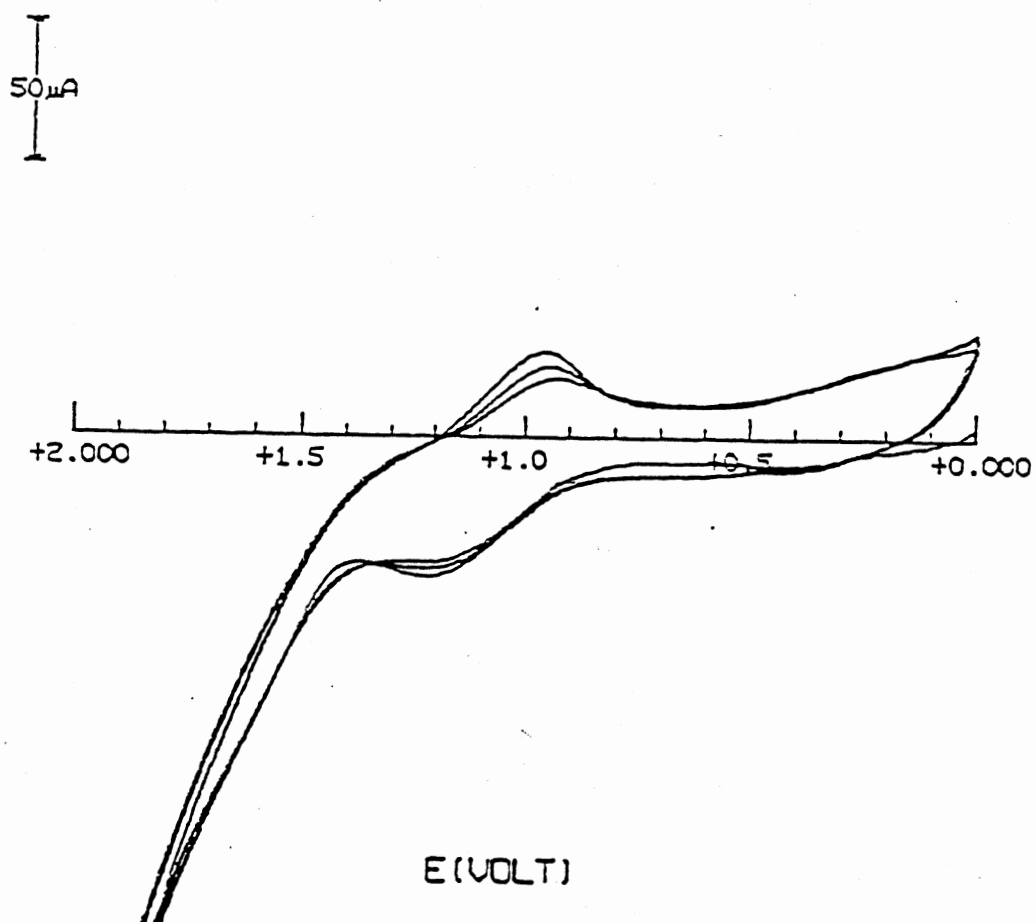


Figure 18. Cyclic Voltammograms of Film-coated Electrode in 0.10 M Picrate Aqueous Solution.

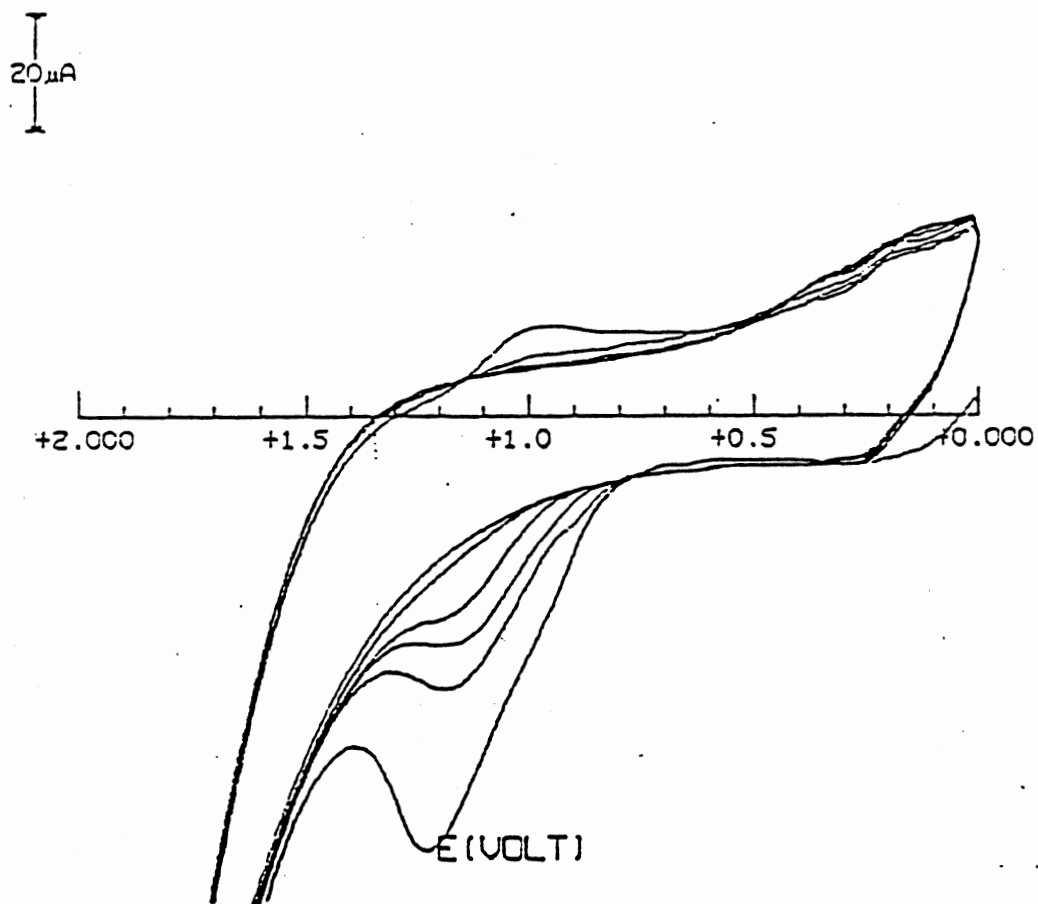


Figure 19. Cyclic Voltammograms of Film-coated Electrode in 0.10 M ClO_4^- Aqueous Solution.

that the electron hopping in the direction of reduction is more difficult than in the opposite direction

(2) Shifts in peak potentials. In an acetonitrile solution 0.10 M in sodium perchlorate, the oxidation peak potential of Fe(II)/Fe(III) redox center on the polymer-modified electrode appears at 1.25 V. This value remains unchanged in most of the supporting electrolyte/water solutions except in formate, acetate, and benzoate solutions. The shifts are about the same in magnitude in the above three cases (see Table 5).

It is not difficult to see the similarities in these three counterions: all of them have carboxylic groups that can interact with the iron center. This means that the carboxylic group must have a special interaction with the redox center inside the polymer, which gives a lower energy barrier to the electron transfer in these systems, so that the oxidation takes place at a lower potential.

Effects in NO₂(g) Detection

In the determination of NO₂(g) the electron transfer process is completed in the following way:

1. NO₂(g) is oxidized at the surface of the polymer.
2. Electron hopping occurs through film.
3. Charge is compensated by counterions.

From those results listed in Table 5, a similar conclusion to those extracted from cyclic voltammetry can be

derived for the counter ion effects in the determination of NO_2 ,

1. Simple ions, such as F^- and Cl^- . The higher the ionic mobility in water, the higher the response.

2. NO_3^- , ClO_3^- , and BrO_3^- . Their ionic mobilities range from 1.915 to 1.49, but the responses are more or less the same.

3. Anions of organic acids. The response decreases with the decreasing of ionic mobility.

Conclusions

From the discussions above, the following are the factors determining the responses observed in cyclic voltammetry and in the NO_2 detection.

1. The geometric structure of the counterion. It is necessary to consider that the geometric structure should affect the diffusion rate of the counterion inside the polymer to a greater extent than in the solution, because of the much more compact structure of the polymer film. Hence, the traditional ionic mobility cannot describe the diffusion rate inside the polymer perfectly. This could be the reason why a bigger signal is obtained for Cl^- than for NO_3^- : the structure of NO_3^- is less compact.

2. The hydration process. The hydration leads to a polymer of less compact structure, and thus a bigger effective separation between redox centers is created. As a

result of this hydration, the current decreases. Generally speaking, the simple ions favor hydration more than inorganic anions containing oxygen, such as NO_3^- . Perchlorate is the least hydrated inorganic anion used here as a counterion and this has been suggested by several other groups [70,71]. Carboxylic anions undergo only mild hydration and the picrate anion is the "driest" among all those tested.

3. The ionic mobility. If the effects of solvation and charge distribution could be eliminated, the response should increase with the increase in ionic mobility; but this can not be verified.

Overall speaking, the process of charge compensation through counter ions does play a significant role in the responses both in cyclic voltammetry and in the NO_2 detection. If it is not the only factor controlling the electron transport rate, at least it part of the factor.

CHAPTER VI

SOME APPLICATIONS OF ELECTRODES MODIFIED

WITH POLYMERIC TRIS[5-AMINO-

1,10-PHENANTHROLINE] IRON[II]

Experimental

Apparatus

The continuous-flow system used included a thin-layer cell with two working electrodes and a reference electrode compartment, with an auxiliary electrode in the form of metal tubing serving also as the exit to waste. This four-electrode arrangement is available from Bioanalytical Systems (West Lafayette, IN) and although it does not compensate significantly for solution resistance, it draws no current through the reference electrode and permits simultaneous responses to be obtained from modified and unmodified working surfaces. A 0.10-mm-thick Teflon spacer provides the gap for passage of solution in the thin-layer cell (see Figure 20).

Gravity flow was used for propulsion of the carrier solution because it provides excellent flow characteristics for electrochemical detection.

The pH was measured with an Orion 601A digital pH meter with an epoxy-body combination electrode.

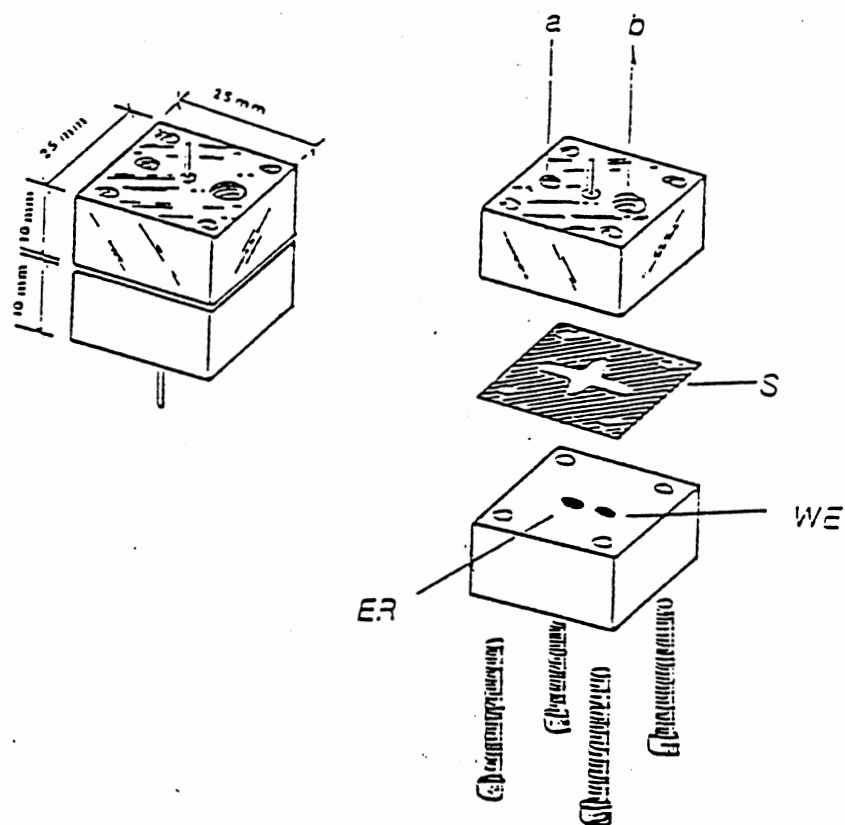


Figure 20. Block Diagram of Thin-layer Cell Machined
 out of Kel-F Material
 WE: Working Electrodes
 S: Teflon Spacer, 0.10 mm thick
 a: Flow in
 b: Flow out
 Distance Between Electrodes: 0.50 mm.

Working electrodes. One of the electrodes had an unmodified surface (see Figure 21) and the second was polymer-modified, this was prepared by performing 122 cycles (at 50 mV/s) between 0 and 1.3 V vs a Ag/AgCl, 3M KCl reference as described in Chapter 3.

Reagents and Solutions

Unless otherwise specified, reagents were of analytical reagent grade. The carrier solution was 0.10 M potassium chloride.

The NO₂(g) was prepared in a gas-tight glass container by exposing a given volume of concentrated nitric acid to sunlight until a constant concentration of NO₂ in the headspace was found (determined by use of sulfanilic acid and N-(1-naphthyl)ethylenediamine dihydrochloride in acetic acid) [74]. The stock NO₂/air mixture, from which dilutions (with air) were made as required, were standardized by the same procedure. The gas sample was introduced from the sample loop of a Rheodyne 4-way valve, filled from a gas-tight Hamilton syringe tightly attached to the entry port.

The phenol stock solutions used as analyte sample were prepared from a "standard" phenol solution (1 ml = 1 mg phenol) obtained from Mallinckrodt, Inc. (Paris, Kentucky). The phenol standard solution was diluted in a 0.10 M KCl solution.

In the determination of phenol, the experimental parameters were as follows:

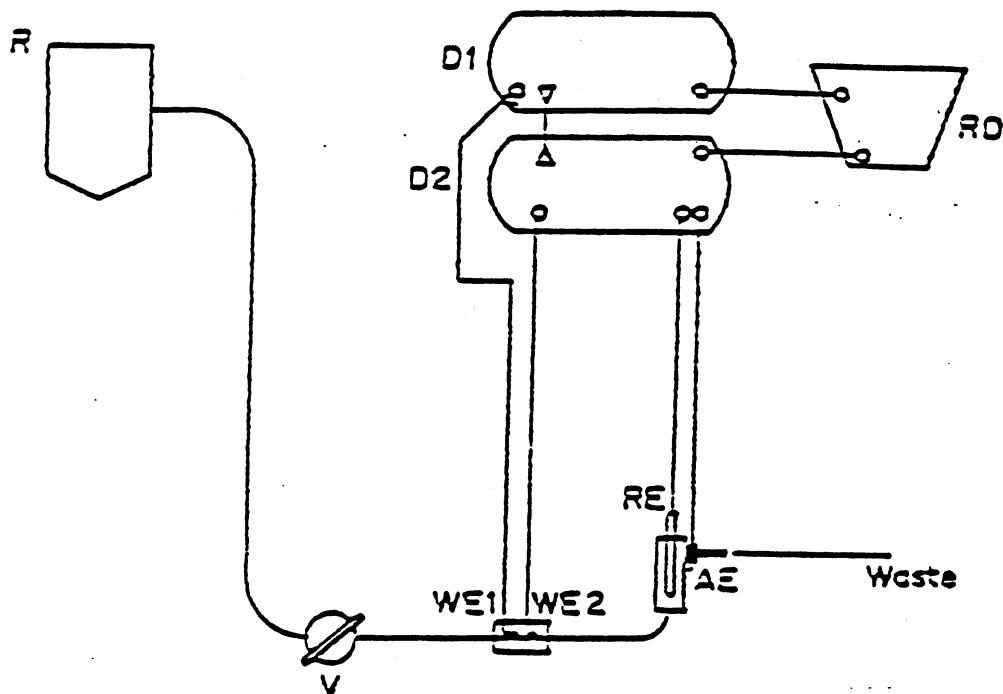


Figure 21. Configuration of Apparatus for Continuous-flow Determinations
 WE1, WE2: Working Electrodes; D1, D2: Amperometric Detectors Connected in Tandem (Model LC4B from Bioanal. Systems)
 RD: Dual-pen Chart Recorder (Model RYT-DB, Bioanal. Systems)
 V: Intercalation Valve (Rheodyne Type 50 4-way Teflon Rotary Valve)
 RE: Reference Electrode (Ag/AgCl, 3M KCl)
 AE: Auxiliary Electrode (Pt wire)
 R: Reservoir with Carrier Electrolyte.

Working potential: 1.000 V.
Flow rate: 6 ml / min.

Results and Discussion

1. Determination of NO₂

I. Response to NO₂. As expected, NO₂(g) readily underwent redox reaction at the immobilized Fe(II)/Fe(III) centers in the polymer-modified electrode. It showed reduction peaks at low positive potentials and oxidation peaks at higher positive potentials, with an "inert" electrochemical behavior at around 0.600 V vs. Ag/AgCl, 3M KCl. Figure 22 shows the hydrodynamic voltammogram for NO₂(g) response. At potentials higher than 1 V, the response reached a plateau, and at this point any potential equal or higher than 1 V could be used for the determination and would give similar sensitivity. When the stability of the signal is considered, the response at 1.00 V gave the best reproducibility, with a relative standard deviation of 6.03% (These results were calculated from 20 injections at each potential). On the other hand, the response at 1.20 V gave a R.S.D. of 8.82%. In the negative direction, the response increases with decreasing potential, but reproducibilities were not as good. At 0.20 V, for example, the R.S.D. was 9.80%. Considering both sensitivity and reproducibility, it was decided to choose a potential of 1.00 V as most suitable for the determination. Also in Figure 21, the difference of responses between the modified and unmodified glassy-carbon

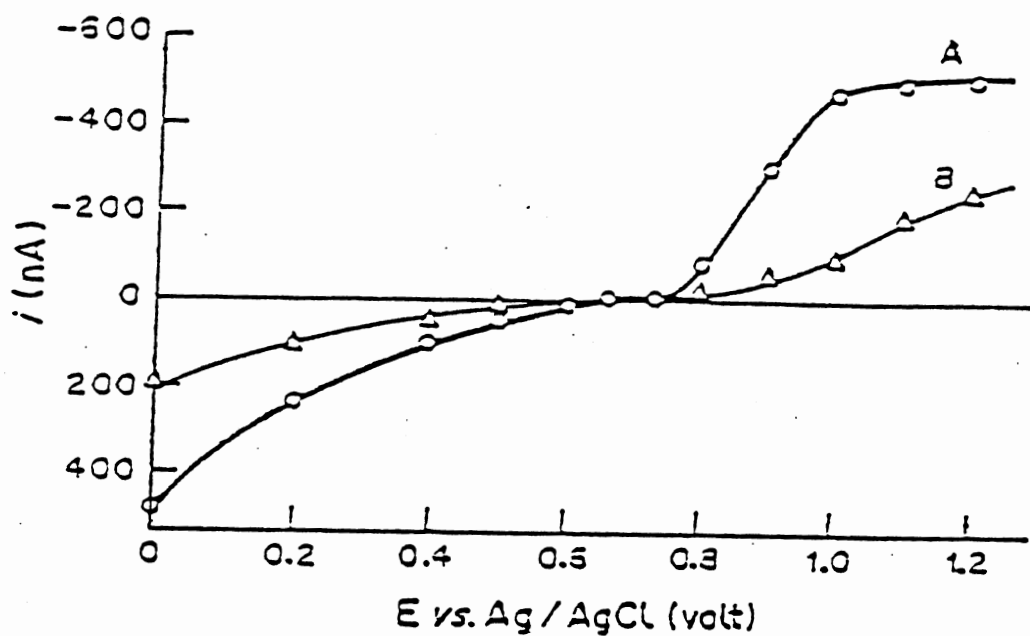
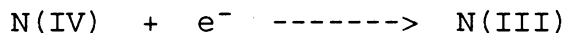


Figure 22. Hydrodynamic Voltammogram Showing the Response to $\text{NO}_2(\text{g})$ at a Concentration of 25.0 ppb(v/v).
A: Response at a Polymer-coated Glassy-carbon Electrode
B: Response at a Naked Glassy-carbon Electrode

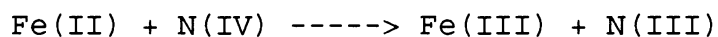
surfaces can be clearly seen. Figure 23 shows typical amperometric signals obtained under continuous-flow conditions and at an applied potential of 1.00 V vs. Ag/AgCl, 3M KCl. The improvement in response at the modified surface realized in this figure is significant.

The chemical and electrochemical reactions that occur at the electrode surface are discussed below.

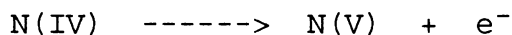
The reduction signals obtained at potentials below 0.600 V at unmodified glassy-carbon electrodes are interpreted as resulting from:



The enhanced response at the polymeric film glassy-carbon electrode does not result from the same reaction, but from a process involving a catalytic cycle:



The oxidation peaks at potentials above 0.600 V at the bare glassy-carbon surface are considered to result from:



and the response at polymer-coated surfaces from:

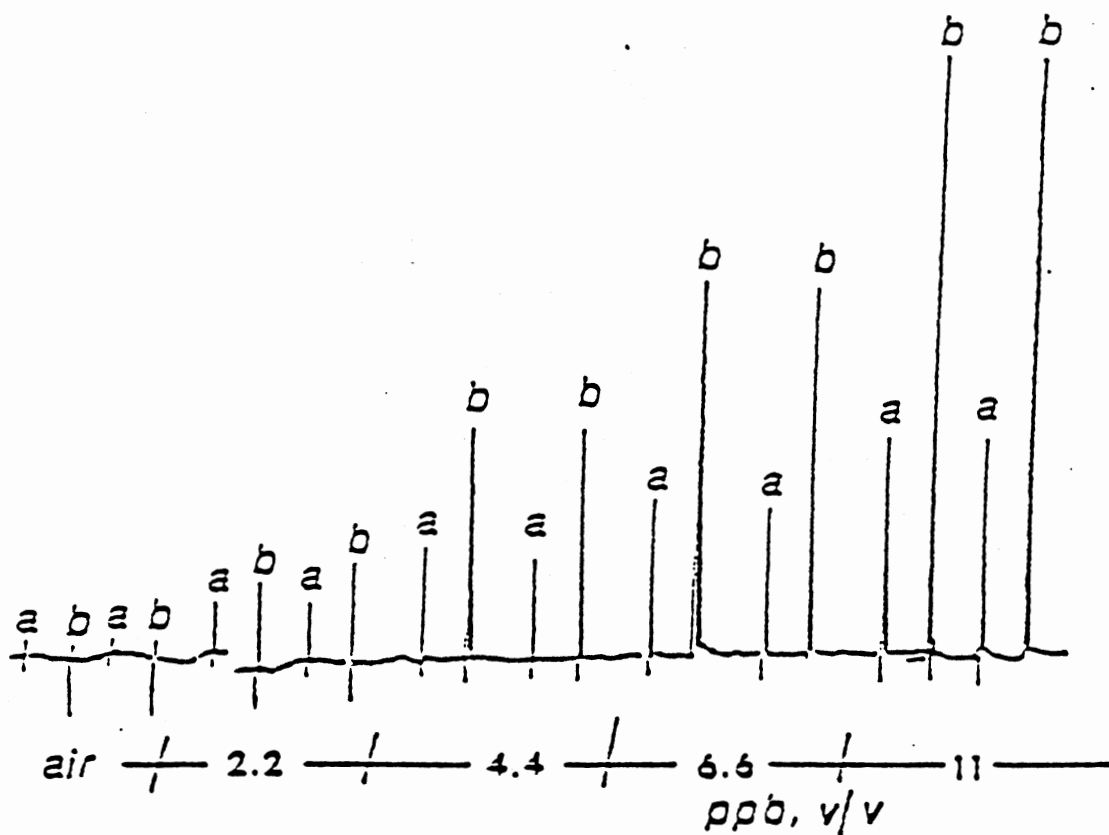
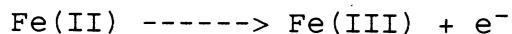
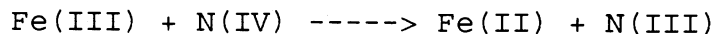


Figure 23. Typical Transient Signals due to $\text{NO}_2(\text{g})$ Injection. Concentration of $\text{NO}_2(\text{g})$ Indicated Below Peaks.
 a: Air Response
 b: Analyte Response



In the case of reduction peaks, the regeneration of Fe(II) on the modified electrode surface triggers the catalytic cycle, which is responsible for the increase in signal compared to that with an unmodified surface. Similarly, in the case of oxidation, the regeneration of Fe(III) initiates the catalytic cycle.

As shown in Figure 24, after the injection of sample, NO₂(g) diffuses onto the electrode surface and gets oxidized or reduced at the surface by Fe(III) or Fe(II) immobilized in the polymeric film. This is followed by electron hopping in the film via redox centers and charge compensation through diffusion of counterions.

II. Effect of Polymer Thickness. The relationship between the thickness of the polymeric layer and the response to NO₂(g) was investigated here. Although the electron hopping in the polymer-coated glassy-carbon electrode is competitively fast [2], a decrease in response would be expected as the number of polymer layers deposited on the surface increases as a result of difficulties with charge compensation. Table 6 includes data verifying this

TABLE 7

RELATIONSHIP BETWEEN THE THICKNESS OF DEPOSITED
POLYMER AND THE RESPONSE OF INJECTED NO₂ (g)

NO ₂ injected (ppb, v/v in air)	No. of Cycles (proportional to thickness of polymer layer)	i_p (nA)
6.4	10	260
	20	220
	30	100

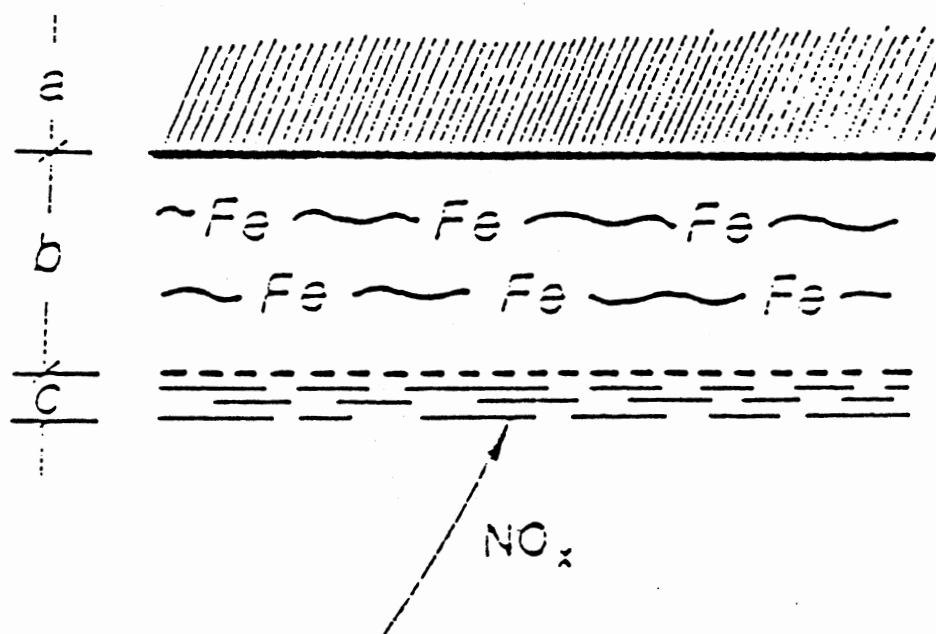


Figure 24. Idealized Structural Representation of the Polymer-coated Glassy-carbon Electrode
 a: Glassy-carbon
 b: Polymer Layer Containing Fe(II)/Fe(III) Centers
 c: Thin Layer of the Electrolyte Solution Bathing the Electrode Surface as a Result of the Imposed Flow.

expectation since reducing the number of cycles used for the electrochemical polymerization results in an increase in signal.

Although a better sensitivity could be obtained from a thinner polymeric layer, we have another factor that needs to be considered: the linear range for determination. Later in the study, it was found that a longer linear range can be obtained with a thicker film coating. Thus, in order to compromise between sensitivity and linear range, an electrode with relatively thick polymer layer was used in determinations. In such a case, the sensitivity is not as high as when a thinner-film electrode is used, but a thicker film increases the concentration range for $\text{NO}_2(\text{g})$ determination. The data illustrating this are shown in the form of a calibration curve in Figure 28.

III. Effect of pH of Carrier Solution. Experiments on the effect of the pH of the carrier solution on the $\text{NO}_2(\text{g})$ response were performed by adjusting the pH with 0.10 M hydrochloric acid or sodium hydroxide solutions. Figure 25 shows the dependence of signal height on pH of the carrier electrolyte solution. From this graph, we can see: increasing the pH makes the response increase until the pH reaches a value about 4.0; at higher pH values the response shows a substantial decrease.

This can be explained in the following manner:

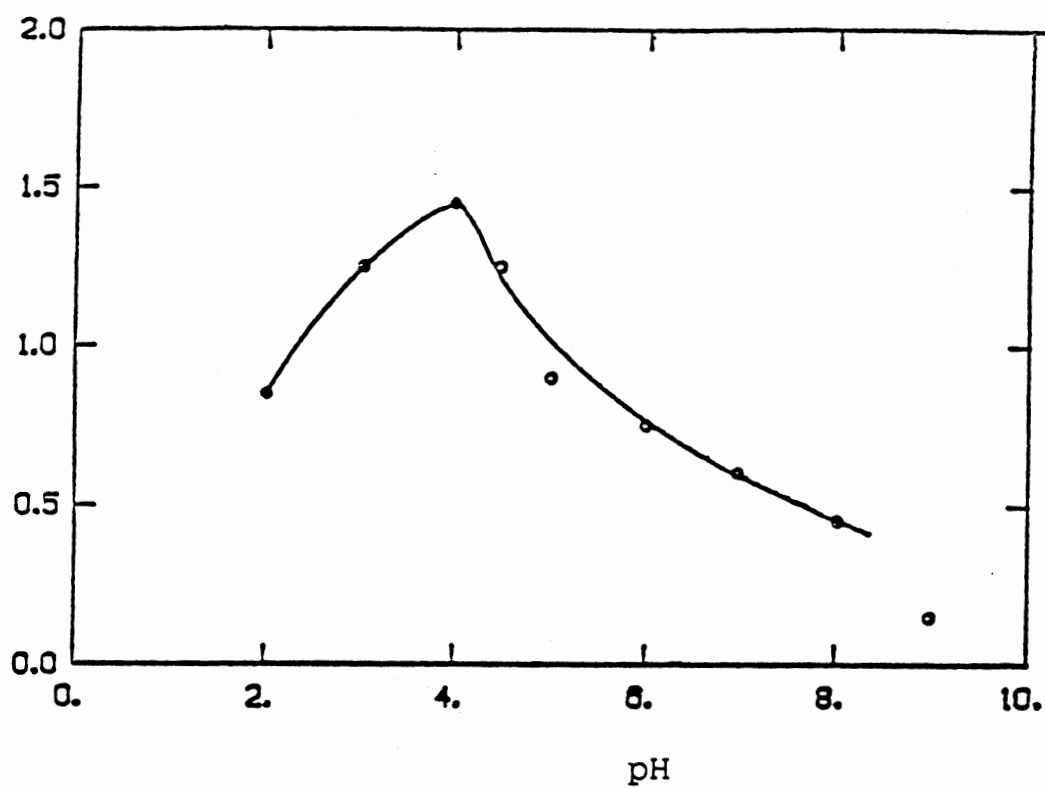
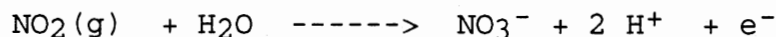


Figure 25. Effect of pH on Signal Height for $\text{NO}_2(\text{g})$ Determination. Concentration of $\text{NO}_2(\text{g})$: 5.5 ppb (v/v in air).

1) Both Fe(II) and Fe(III) have very strong complexing ability with the OH⁻ ion, so with an increase in pH, the OH⁻ becomes more and more competitive with the original ligand for the iron. As a result of this competition, the OH⁻ replaces the original ligands in the complex to a certain extent and the formal potential of the new complex shifts to a different value, which causes the response to NO₂(g) to decrease with an increase in pH (after pH=4.00).

2) As shown earlier, the response of NO₂(g) is due to the conversion of N(IV) to N(V), and most likely, the reaction shown below actually occurs:



Since protons are a product of this reaction, a basic medium would favor it. Consequently, the higher the pH, the higher is the response that should be expected.

As a result of the above two factors, at lower pH values the second factor is predominant, but at higher pH values the first factor is in control. This is why a bell-shaped curve is obtained. In conclusion, a pH of about 4.00 is recommended for the determination of NO₂(g).

IV. Effects of Carrier Flow Rate and Injected Sample Size. The carrier flow rate is another important factor in the operation of a continuous-flow system. From a theoretical point of view, the slower the flow, the more time

would the sample have for contact with the electrode surface and an enhanced response should be expected. In actuality, however, a low flow rate results in an undesired consequence: peak broadening. This is caused by a much more serious dispersion of the injected sample when a slower flow is adopted, and this peak broadening affects the sensitivity to a certain degree as well as decreases the rate of sample injection. In order to compromise between sensitivity and peak shape, a new parameter was adopted as a standard to dictate the effect of flow rate; such a parameter can be defined as follows:

$$R = \underline{i}_p / \underline{w}(t),$$

where \underline{i}_p is the peak height in nA and $\underline{w}(t)$ is the peak width in unit of time (second). The units of R are nA/s.

The flow rate that corresponds to the largest value of R is considered to be the optimum. In such a case, the signal will be as high as possible under the condition of smallest peak broadening possible. In Figure 26 the corresponding experimental results are shown.

Hence a flow rate of about 5-7 ml/min is recommended; this provides an injection rate of 100-200 samples per hour.

Ideally, in a flow injection determination the response to the analyte should be proportional only to the concentration of analyte; the sample size should not affect

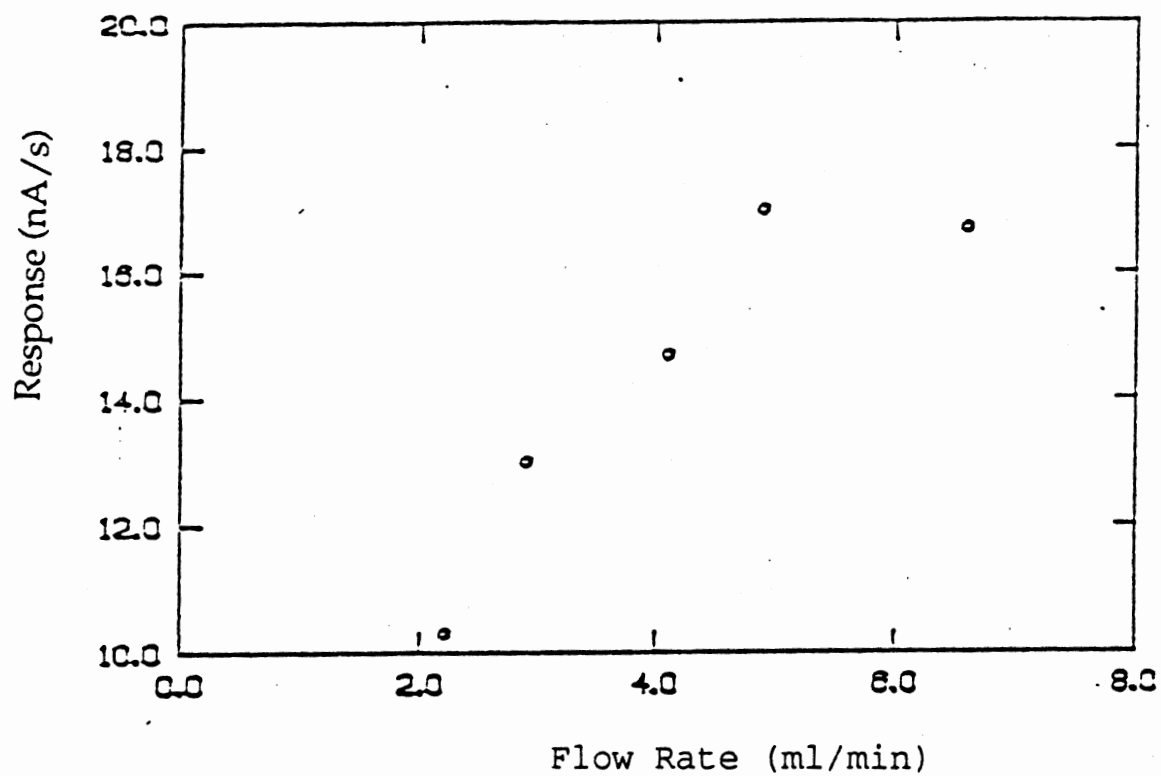


Figure 26. Effect of Carrier Flow Rate on Signal Height for NO₂(g) Determination.
Concentration of NO₂(g):
5.5 ppb (v/v in air).

the response at all. But in the actual operation, a change in response with different sample size is observed. This is probably due to relatively more diffusion of the sample into the carrier solution when the sample is small. Figure 27 presents the corresponding experimental observations. When the sample size is too small, the response is not as good as when a larger sample is used. On the other hand, a very large sample size results in unnecessary waste. Generally, a sample size of about 200-400 μl can be considered acceptable for practical purposes.

V. Sensitivity, Limit of Detection, Dynamic Range and Stability. The slopes of the calibration curves shown in Figure 28 define method sensitivity. The polymer-film modified electrode exhibits very good sensitivity. It also offers good linearity. As mentioned earlier its sensitivity, however, is a function of the number of layers deposited on the conducting surface and hence which is determined by the number of cycles applied in the electropolymerization process). The value of 18 nA/ppb (v/v) was obtained with an electrode modified by using 122 cycles. If only 20 cycles are used, the sensitivity improves to 21.3 nA/ppb (v/v), but the linear dynamic range is reduced to about 10 ppb (v/v). The limit of detection, calculated as the concentration corresponding to the blank (air) signal plus three times the standard deviation of this blank, is about 2 ppb (v/v). Figure 24 also shows the response to $\text{NO}_2(\text{g})$ at a bare glassy-

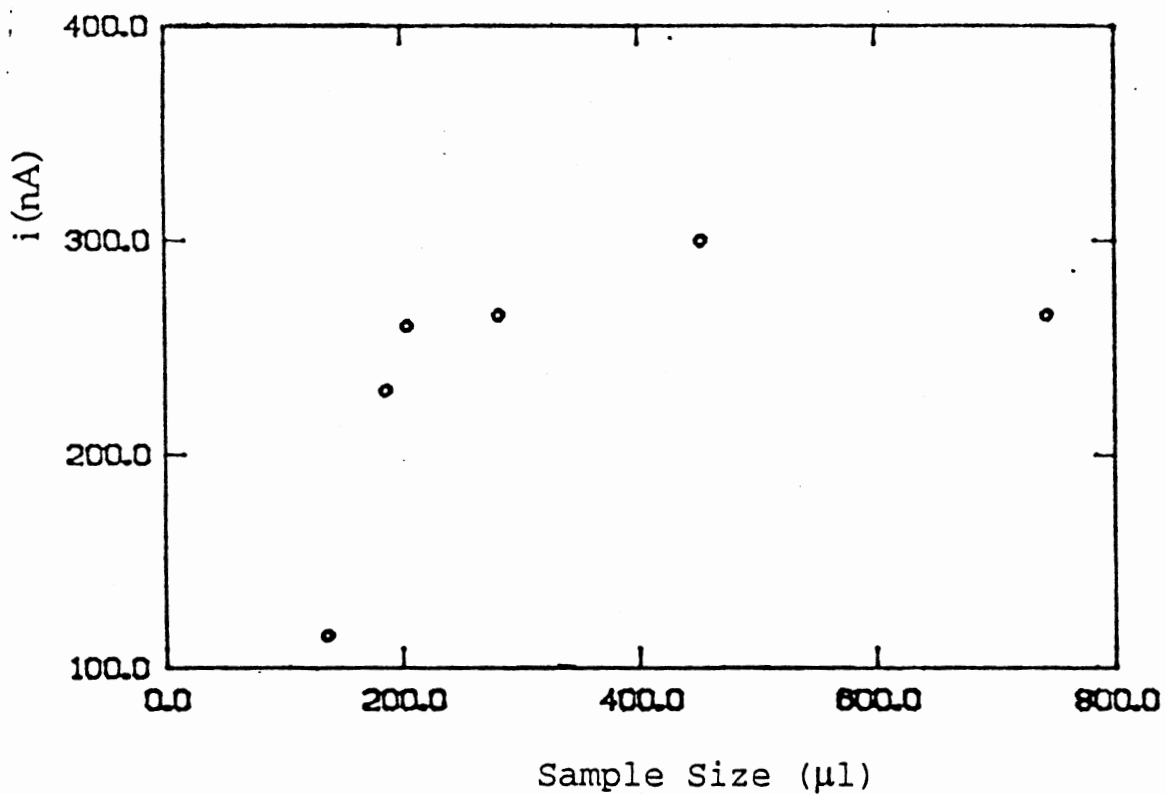


Figure 27. Effect of Sample Size on Signal Height for $\text{NO}_2(\text{g})$: Determination
Concentration of $\text{NO}_2(\text{g})$: 5.5 ppb
(v/v in air).

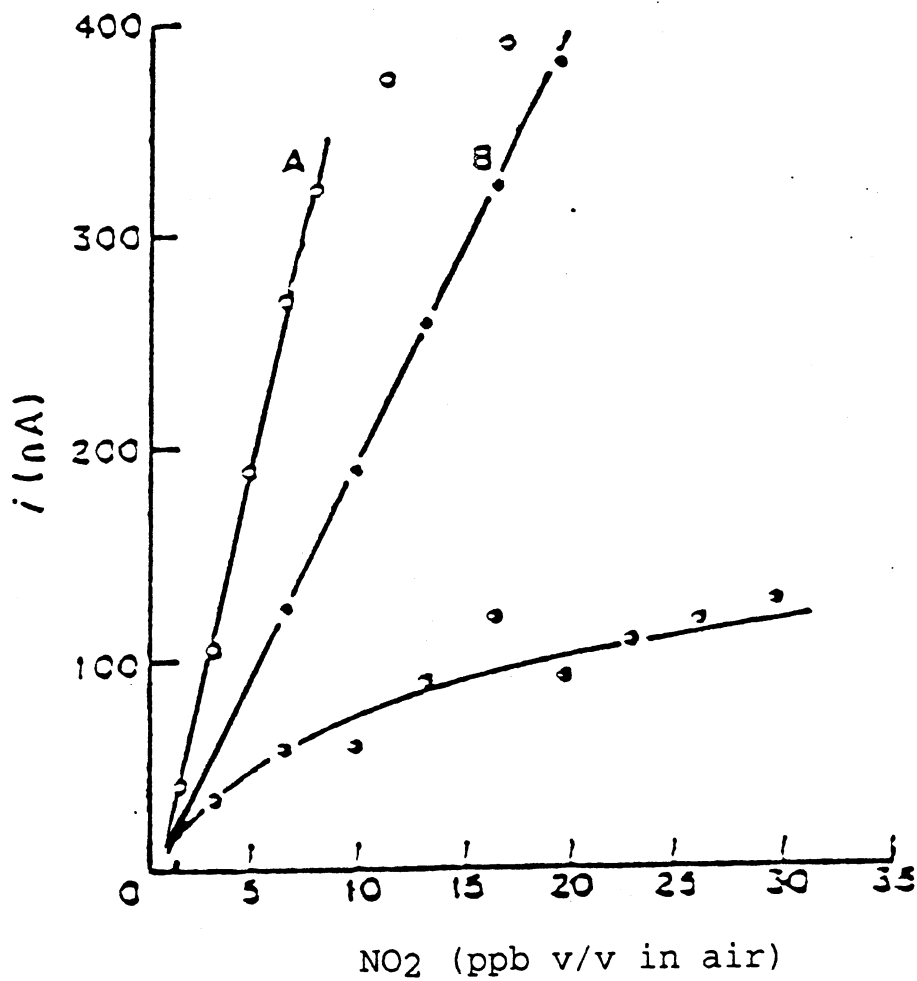


Figure 28. Dependence of Signal Height on $\text{NO}_2(\text{g})$ Concentration
A: Polymer-coated Glassy-carbon Electrode Prepared with 10 Cycles
B: Polymer-coated Glassy-carbon Electrode Prepared with 120 Cycles
C: Bare Glassy-carbon Electrode

carbon electrode. The poisoning of the bare surface and consequently the inadequacy of its use for $\text{NO}_2(\text{g})$ determination, after a few injections, can be clearly seen.

Table 7 shows typical data illustrating the good short-term stability of the polymer-coated glassy-carbon electrode in continuous-flow operation.

The electrode could be stored in air or in supporting electrolyte without any significant difference in its performance. There was no significant deterioration in signal from surfaces used for detection up to 7 continuous hours or more than one month of intermittent use. The relative standard deviation (typically 5%) is mainly the result of uncertainties arising from the mode of injection.

2. Determination of Phenol, SO_2 , H_2S , and Cl_2 .

Response to Phenol

Phenol can be electrochemically oxidized on a carbon paste or carbon electrode at a relatively high potential. Because of the rapid fouling of the electrode surface by the deposition of a polymeric film produced by phenolate ion [76], however, the glassy-carbon electrode can not be conveniently used for the determination of phenol.

In a preliminary test, the electrode coated with tris[5-amino-1,10-phenanthroline]iron[II] polymer film exhibited a

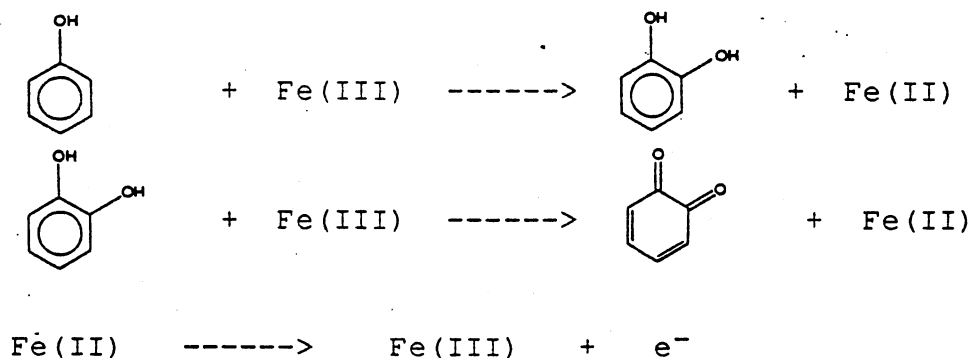
TABLE 7

REPETITIVE RESPONSE OF A POLYMER-MODIFIED
ELECTRODE TO 18 ppb (v/v) NO₂

Age of electrode	\bar{i} (nA)	No. of determinations
Freshly prepared	325±12	10
1 h	338±10	10
2 h	338±13	10
3 h	346±15	8
24 h	353±3	3
3 months	deterioration 5%	

* Electrode kept in contact with supporting electrolyte between runs.

very good response towards phenol. This response should be generated by the oxidation of the phenol.



The method also shows good reproducibility. The limit of determination is obtained as 6 ng/mg with a linear range of $4 - 10^4$ ng / ml. The calibration curve is shown in Figure 29,30.

In comparison with previous work done in our group on the determination of phenol [76], this method with the application of a polymer-film-coated glassy-carbon electrode offered a very competitive limit of determination, 6 ng / ml, while the other gave a limit of detection of 18 ng /ml with a linear range less than 10 ng / ml.

Response to Halogens

While response to chlorine gas was easily reproduced, $\text{I}_2(\text{g})$ and $\text{Br}_2(\text{g})$ gave very irreproducible responses, with apparent destruction of the tris[5-amino-1,10-phenanthroline]iron[II] polymeric films on the electrode surfaces.

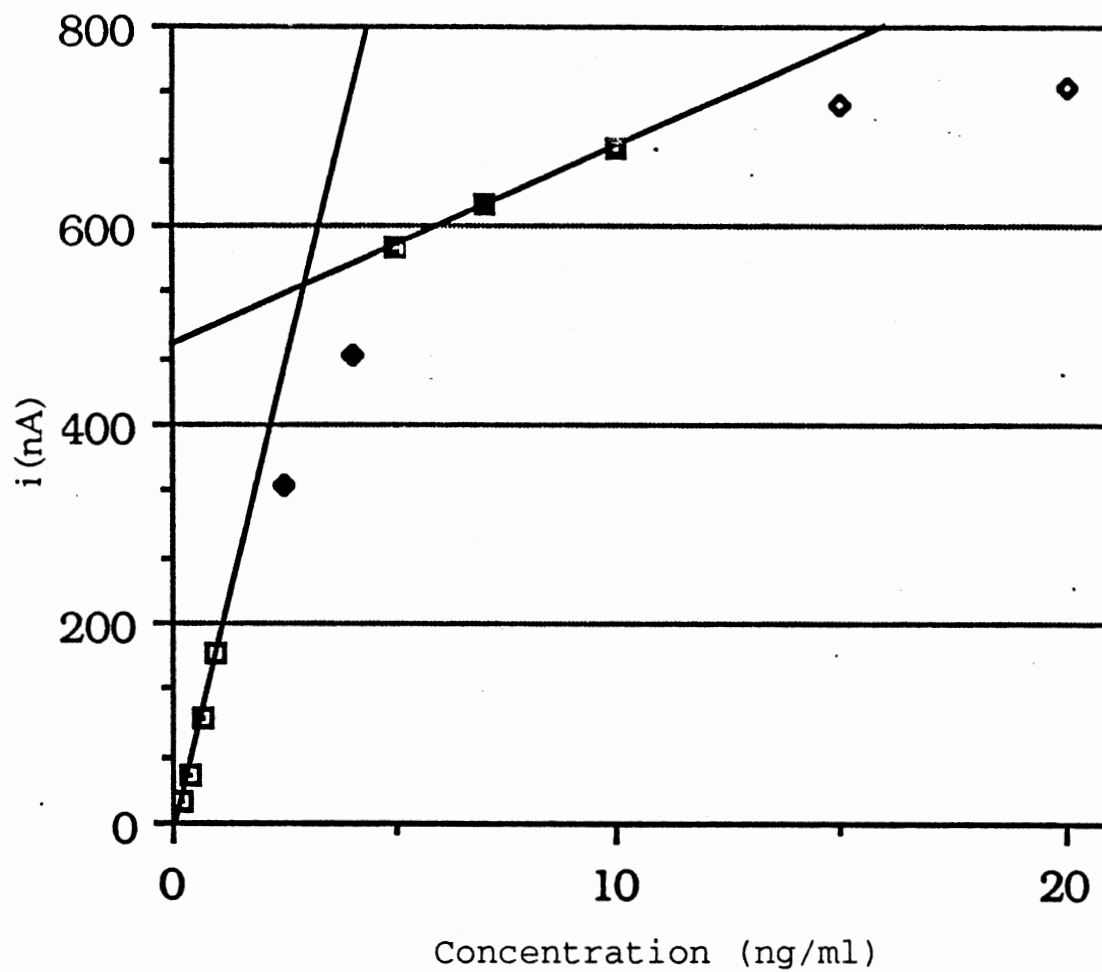


Figure 29. Calibration Curve for Phenol
Determination on Modified
Glassy-carbon Surfaces

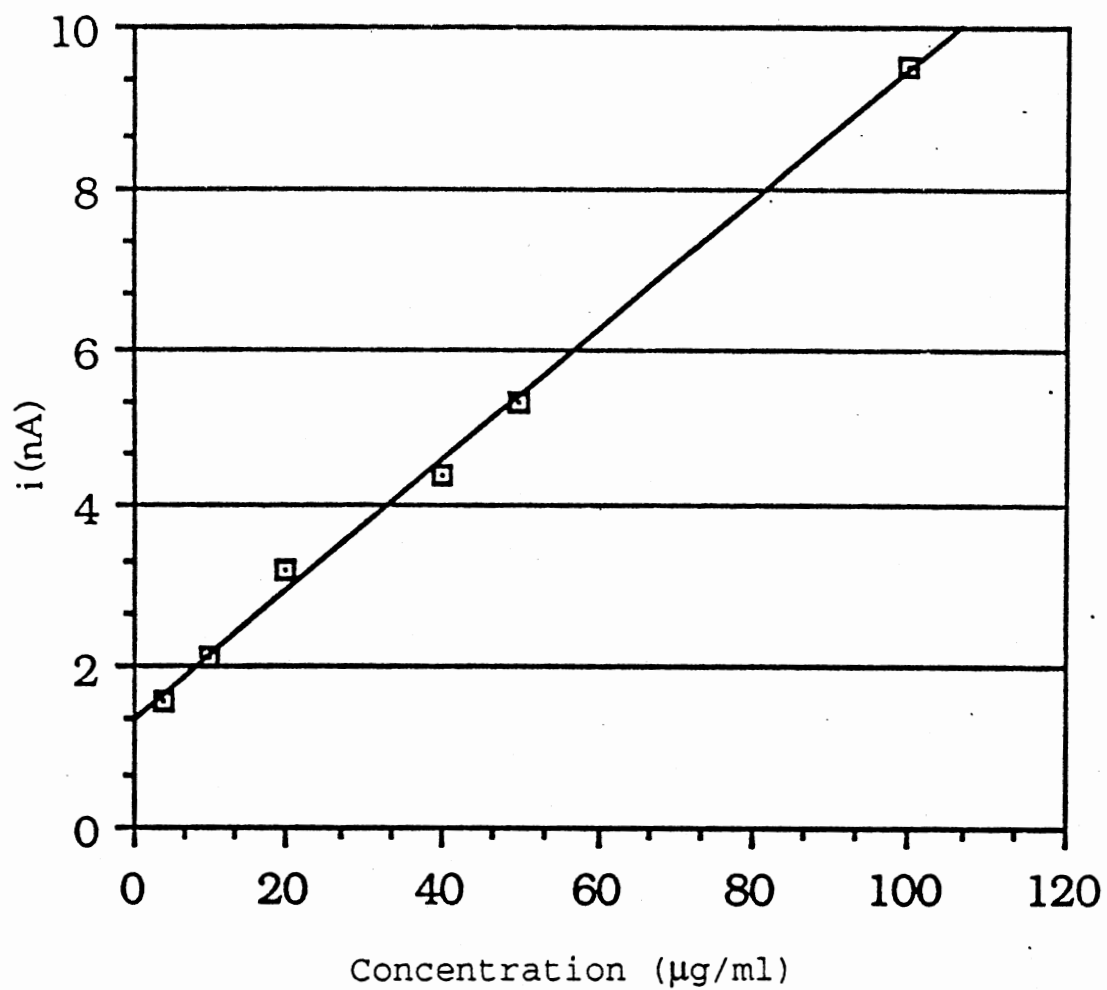


Figure 30. Calibration Curve for Phenol
Determination on Modified
Glassy-carbon Surfaces

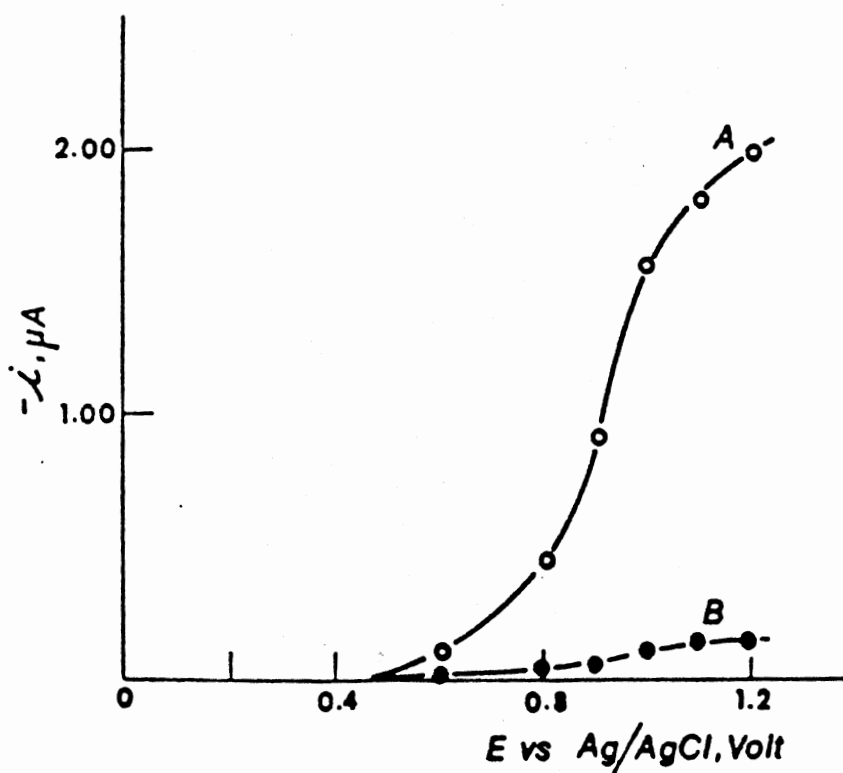


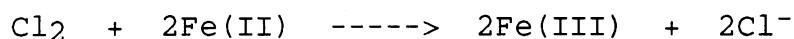
Figure 31. Hydrodynamic Voltammogram for $Cl_2(g)$ (1 ppm v/v in air). (A) Response at a Polymer-coated Glassy-carbon Electrode, (B) Response at a Naked Glassy-carbon Electrode. Supporting Electrolyte, 0.10 M KCl (pH = 4.00); Flow Rate, 2.0 ml/min; Injected Sample Size, 250 μl .

Chlorine response is illustrated in Figure 31 in the form of a hydrodynamic voltammogram. Only reduction peaks were observed on both the glassy-carbon surface and the modified glassy-carbon surface in the range of potential tested. Interpretation of these responses is as follows:

at glassy-carbon surface:



at modified surface:

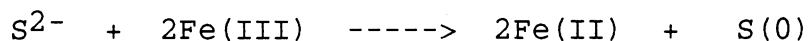


The maximal signal height was obtained at about +0.6 V. The pH of the carrier affected the signal height; the optimum pH was about 4.0.

Response to Sulfur Dioxide and Hydrogen Sulfide Gases

Figures 32, and 33 are the hydrodynamic voltammograms showing the responses to $\text{H}_2\text{S(g)}$ and $\text{SO}_2(\text{g})$. The oxidation currents on the modified surfaces are considered to result from the following reactions:

For H_2S :



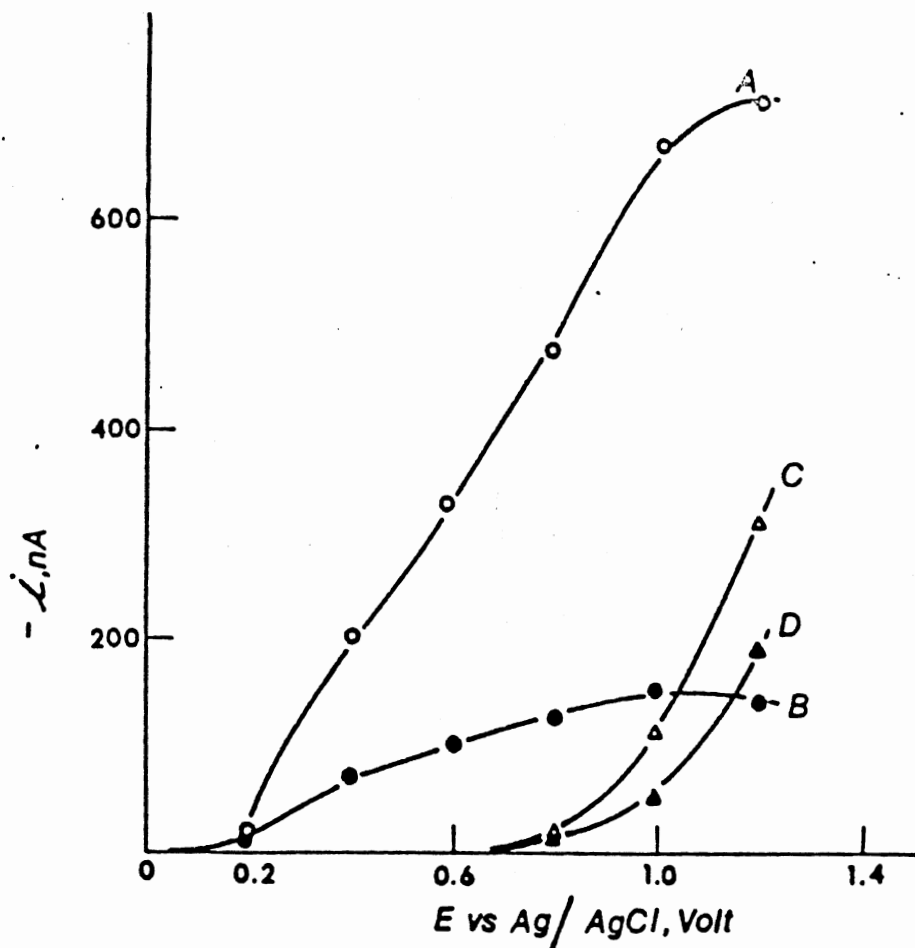


Figure 32. Hydrodynamic Voltammogram for $H_2S(g)$, 4.76 ppm v/v. (A) Response at a Polymer-coated Glassy-carbon Electrode, (B) Response at a Naked Glassy-carbon Electrode. (C) Response at a Carbon Paste Chemically Modified by incorporation of 10% w/w Tris[4,7-diphenyl-1,10-phenanthroline]iron(II) Perchlorate, (D) Response at an Unmodified Carbon Paste Electrode. Experimental Conditions as in Fig. 31.

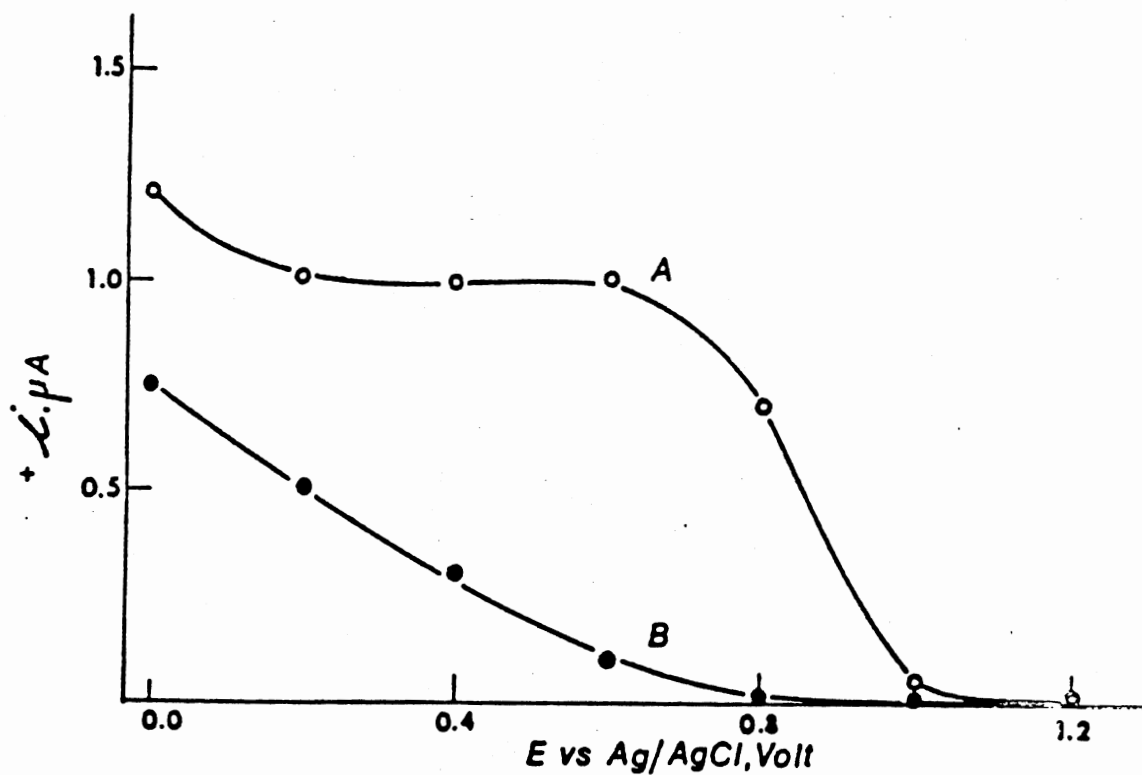
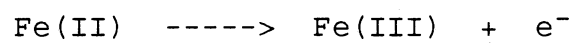
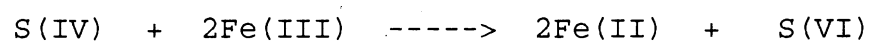


Figure 33. Hydrodynamic Voltammogram for SO₂(g), 3.96 ppm v/v in air. (A) Response at a Polymer-coated Glassy-carbon Electrode, (B) Response at a Naked Glassy-carbon Electrode. Experimental Conditions as in Fig. 29.

For SO₂:



In both cases, pH of about 4.0 gave the highest responses.

CHAPTER VII

CONCLUSIONS

This research project basically consisted of the following three parts. The first part dealt with the electrochemical polymerization and some characterization of the polymeric film prepared by cyclic voltammetry of tris[5-amino-1,10-phenanthroline]iron[II] complex using UV-visible, infrared spectra and electron scanning microscopy. The possible structure of the polymer formed by electrochemical polymerization was thus identified.

The second part was dedicated to the evaluation of counter-ion effects both by cyclic voltammetry and by detection of $\text{NO}_2(\text{g})$ with the hope of finding out the rate limiting factor in the electron transport process. It was concluded that the charge compensation through counter-ion motion does play a significant role in electron transport through the polymer film and the responses increase with increase in the ionic mobility for anions with similar structure. In addition, the collected observations also gave valuable reference for the selection of supporting electrolytes in the determination of certain analytes.

The third part was devoted to the application of modified electrodes of the type studied as amperometric detectors. The determination of $\text{NO}_2(\text{g})$, phenol, $\text{Cl}_2(\text{g})$,

H₂S(g), SO₂(g) was performed in a continuous-flow processing system with the tris[5-amino-1,10-phenanthroline]Fe[II] polymeric film-coated glassy-carbon electrode as detector. This type of electrode proved to be a very sensitive and long lasting sensor, especially for NO₂(g) and phenol. The limit of detection for NO₂ can be at the ppb level, one of the lowest so far reported. Some experimental parameters like pH, flow rate and sample size were optimized for the NO₂(g) detection.

REFERENCES

- Kolthoff, I. M., Lingane, J. J., Polarography,
Interscience, New York, 1952.
2. Murray, R. W., Electroanalytical Chemistry,
Bard, A. J. (ed.), Marcel Dekker, New York, 1984,
Vol. 13.
 3. Kamau, G. N., Willis, W. S., and Rusling, J. F.,
Anal. Chem., 57, 545 (1985).
 4. Burns, E. A., The Analytical Chemistry of Nitrogen and
Its Compound, Streuli, C. A. and Averel, P. R. (eds.),
Wiley-Interscience, New York, 1970.
 5. Fox, D. L., Anal. Chem., 57, 223R (1985).
 6. Idem, *ibid.*, 59, 280R (1987)
 7. Bergman, J. Electroanal. Chem., 157, 59 (1983).
 8. Faulkner, L. R., Electrochim Acta, 34, 1699 (1989).
 9. Lane, R. F. and Hubbard, A. T., J. Phys. Chem.,
77, 1401 (1973).
 10. Moses, P. R., Wier, L., and Murray, R. W., Anal. Chem.,
47, 1882 (1975).
 11. Murray, R. W., Ewing, A. G., and Durst, R. A.,
Anal. Chem., 59, 379A (1987).
 12. Chidsey, C. D. E. and Murray, R. W., Science,
231, 25 (1986)
 13. Collman, J. P., Denisevich, P., Konal, Y., Morroco, M.,
Koval, C., and Anson, F. C., J. Am. Chem. Soc.,
102, 6067 (1983).
 14. Tomi, T. T., Liu, H. Y., and Weaver, M. J.,
J. Am. Chem. Soc., 106, 1233 (1984)
 15. Albery, J. W., Eddowes, M. J., Hill, H. A. O.,
and Hiiman, A. R., J. Am. Chem. Soc., 103, 3904 (1981)

16. Lenhard, J., R., Rocklin, R. Abruna, H., William, K., Kuo, K., and Murray, R. W., *J. Am. Chem. Soc.*, 100, 7870 (1978).
17. Tse, D. C. S., and Kuwana, T., *Anal. Chem.*, 50, 1315 (1978).
18. Frazier, W. M., and Mottola, H. A., *J. Electroanal. Chem.*, 239, 175 (1988).
19. Hurrell, H. C., Abruna, H. D., *Inorg. Chem.*, 29, 736 (1990).
20. Grepouri, I. D., Bedioui, F., and Devynck, J., *J. Electroanal. Chem.*, 238, 197 (1987).
21. Ellis, C. D., Margerum, L. D., Murray, R. W., and Mayer, T. J. *Inorg. Chem.*, 22, 1283 (1983).
22. Dunsch, L., Kavan, L., and Weber, J., *J. Electroanal. Chem.*, 280, 313 (1990).
23. Cosnier, S., Deronzier, A., Moutet, J. C., and Roland, J. F., *J. Electroanal. Chem.*, 271, 69 (1989).
24. Bartlett, P. N., Chung, L. Y., and Moore, P., *Electrochim Acta*, 35, 1273 (1990).
25. Baldwin, R. P., Christensen, J. K., and Kyger, L., *Anal. Chem.*, 58, 1790 (1986).
26. Ghosh, P. K. and Bard, A. J., *J. Am. Chem. Soc.*, 105, 5691 (1983).
27. Murray, C. J., Nowak, R. J., and Rolison, D. R., *J. Electroanal. Chem.*, 164, 205 (1984).
28. Miller, L. L. and Van De Mark, M. R., *J. Am. Chem. Soc.*, 100, 639 (1978).
29. Daum, P. and Murray, R. W., *J. Phys. Chem.*, 85, 389 (1981).
30. Merz, A. and Bard, A. J., *J. Am. Chem. Soc.*, 100, 3222 (1978).
31. Schroeder, A. H. and Kaufman, F. B., *J. Electroanal. Chem.*, 113, 209 (1980).
32. Daum, P. and Murray, R. W., *J. Electroanal. Chem.*, 103, 289 (1979).

33. Barbero, C., Silber, J. J., and Sereno, L.,
J. Electroanal. Chem., 291, 81 (1990).
34. Inzelt, G., Chambers, J. Q., Kistel, J. F., and Day, R.
W., J. Am. Chem. Soc., 106, 3396 (1984).
35. Pickup, F. G. and Osteryoung, R. A.,
J. Electroanal. Chem., 195, 271 (1985).
36. Patil, A. O., Heeger, A. J., and Wudl, F., Chem. Rev.,
88, 183 (1988).
37. Mubarak, M. S. and Peters, D. G., J. Electroanal. Chem.,
273, 283 (1989).
38. Fan, R. F., and Bard, A. J., J. Electroanal. Soc.,
133, 301 (1986).
39. Penner, R. M. and Martin, C. R., J. Electroanal. Soc.,
133, 310 (1986).
40. Bidan, D., Deronzier, A., and Moutet, G. C.,
N. J. Chim., 8, 501 (1984).
41. Cosnier, S., Deronzier, A., and Moutet, G. C.,
J. Electroanal. Chem., 193, 193 (1985).
42. Bedioui, F., Merino, A., Devynck, J., Mestres, C. E.,
and Bied-Charreton, C., J. Electroanal. Chem.,
239, 191 (1988).
43. Moisy, P., Bedioui, F., Robin, Y., and Devynck, J., J.
Electroanal. Chem., 250, 191 (1988).
44. Deronzier, A. and Latour, J. M., J. Electroanal. Chem.,
224, 295 (1987).
45. Dair, F., Bedioui, F., Devynck, J.,
and Bied-Charreton, C., J. Electroanal. Chem., 224, 95
(1987)
46. Armengaud, C., Moisy, P., Bedioui, F., Devynck, J., and
Bied-Charreton, C., J. Electroanal. Chem.,
277, 197 (1990).
47. Dire, F., Bedioui, F., Devynck, J., and Bied-Charreton,
C., J. Electroanal. Chem., 205, 309 (1986).
48. Bidan, G., Dvisia Blohorn, B., Kern, J. M., and
Sauvage, J. M., J. Chem. Soc. Chem. Commun.,
723 (1988).

49. Eaves, J. G., Munro, H. S., and Parker, D.,
J. Chem. Soc. Chem. Commun., 684 (1985).
50. Eaves, J. G., Munro, H. S., and Parker, D.,
Inorg. Chem., 26, 644 (1987).
51. Cosnier, S., Deronzier, A., and Moutet, J. C.,
J. Electroanal. Chem., 207, 315 (1986).
52. Elliott, C. M., Balby, C. J., Nuwaysir, L. M.,
and Wilkins, C. J., Inorg. Chem., 29, 389 (1990).
53. Denisevich, P., Abruna, H. D., Leidner, C. R.,
Meyer, T. J., and Murray, R. W., Inorg. Chem.,
21, 2153 (1982).
54. Calvert, J. M., Schmehl, R. H., Sullivan, B. P.,
Fassi, J. S., T. J., and Murray, R. W., Inorg. Chem.,
22, 2151 (1983).
55. Ghosh, P. K. and Spiro, T. G., J. Am. Chem. Soc.,
102, 5543 (1980).
56. Leidner, C. R. and Murray, R. W., J. Am. Chem. Soc.,
106, 1606 (1984).
57. Pickup, P. G., Kutner, W., Leidner, C. R.
and Murray, R. W., J. Am. Chem. Soc., 103, 1991 (1984).
58. Abruna, H. D., Denisevich, P., Umana, M., Meyer, T. J.,
and Murray, R. W., J. Am. Chem. Soc., 103, 1 (1981).
59. Denisevich, P. Willman, K., and Murray, R. W.,
J. Am. Chem. Soc., 103, 4727 (1982).
60. Bettelheim, A., Write, B. A., and Murray, R. W.,
J. Electroanal. Chem., 217, 271 (1987).
61. Pham, M. C., Lacaze, P. C., and Dubois, J. E.,
Bull. Soc. Chim. Fr., 2, 162 (1986).
62. Pickup, P. G. and Osteryoung, R. A., Inorg. Chem.,
24, 345 (1985).
63. Genies, E. M., Tsintavis, C., J. Electroanal. Chem.,
200, 127 (1986).
64. Volkov, A., Tourillon, G., Lacaze, P., and Dubois, J.,
J. Electroanal. Chem., 115, 279 (1980).
65. Daum, P., Lenhard, J. R., Rolison, D. R.,
and Murray, R. W., J. Am. Chem. Soc., 102, 4649 (1980).

66. Oyama, N. and Anson, F. C., *J. Electrochem. Soc.*, 127, 640 (1980).
67. Hurrell, H. C. and Abruna, H. D., *Inorg. Chem.*, 29, 736 (1990).
68. Inzelt, G., Fekete, E., and Szabo, L., *Acta Chim. Hung.* 125, 435 (1988).
69. Oh, S. and Faulkner, L. R., *J. Am. Chem. Soc.*, 111, 5613 (1989).
70. Oh, S. and Faulkner, L. R., *J. Electroanal. Chem.*, 269, 77 (1989).
71. Doblhofer, K. and Kappadonia, M., *Colloids and Surfaces*, 41, 211 (1989).
72. Inzelt, G., *Acta Chim. Hung.*, 122, 187 (1986).
73. Inzelt, G. and Bacskai, J., *Acta Chimica Hungarica*, 125, 75 (1988).
74. Boltz, D. F. and Taras, M. J., *Colorimetric Determination of Nonmetals*, 2nd Ed., Boltz, D. F. and Howell, J. A. (eds.), pp 241, Wiley-Interscience, New York, 1978.
75. Kortum, G. and Bockis, J. O'M., *Textbook of Electrochemistry*, Elsevier Publishing Company, 1951.
76. Zacaria, K., Ph.D Thesis, 1990.
77. Oyama, N; Anson, F. C., *J. Electrochem. Soc.*, 127, 147 (1980).
78. Inzelt, G., *Electrochim. Acta*, 83, 34 (1989).
79. Inzelt, G; Szabo, L., *Electrochim. Acta*, 31, 1381 (1986).
80. Inzelt, G; Szabo, L.; Chambers, J. Q.; Day, R. W., *J. Electroanal. Chem.*, 242, 265 (1988).
81. Bonakdar, M.; Mottola, H. A., *Anal. Chim. Acta*, 224, 305 (1989)

VITA²

JIANBO YU

Candidate for the Degree of

DOCTOR OF PHILOSOPHY

Thesis: ELECTROCHEMICAL STUDIES AND APPLICATIONS OF TRIS
[5-AMINO-1,10-PHENANTHROLINE]Fe[II] POLYMERIC-FILM-
COATED GLASSY-CARBON ELECTRODES

Major Field: Chemistry

Biographical:

Personal Data: Born in Shandong, P. R. China,
December 17, 1963, the daughter of Jingchao Yu
and Guiqing Pai.

Education: Graduated from the First High School of
Laiyang, Shandong, in July 1980; Received Bachelor
of Science Degree in Chemistry from Shandong
University in July, 1984; Completed requirements for
the Doctor of Philosophy Degree at Oklahoma State
University in July, 1991.

Professional Experience: Teaching Assistant & Research
Assistant, Department of Chemistry, Oklahoma State
University, January, 1988, to December, 1990;
Teacher, Department of Chemistry, Shandong
University, July, 1984, to April, 1987.